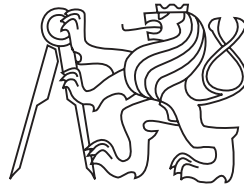


**Czech Technical University in Prague**  
**Faculty of Nuclear Sciences and Physical Engineering**

**Department of Physics**



**Simulations of magnetic equilibrium in  
tokamaks**

**DIPLOMA THESIS**

Author: Martin Matušů  
Supervisor: Ing. Jakub Urban, Ph.D.  
Year: 2017

Insert ASSIGNMENT here.

## **Declaration**

I hereby state that I have written this diploma thesis on my own and used only informational materials mentioned in attached list.

I agree with using this work in the meaning of the Act §60 No.121/2000 Coll., i.e. of Author's law.

Done in Prague, 6 January 2017.

.....  
Martin Matušů

## **Acknowledgement**

I would like to express my deep gratitude to the supervisor of this work Jakub Urban, Ph.D. for his infinite patience and time variability as well as for his guidance and widening of my knowledge in the topic. I would also like to thank Ing.Martin Imříšek for providing results of his simulations as input data for COMPASS-U modelling part of this work.

Last but not least important, I owe more than thanks to my family members for their psychological and financial support during my university studies.

Martin Matušů

*Název práce:*

## **Simulace magnetické rovnováhy tokamaků**

*Autor:* Martin Matušů

*Obor:* Fyzika a Technika Termojaderné Fúze

*Druh práce:* Diplomová práce

*Vedoucí práce:* Ing. Jakub Urban, Ph.D.  
Ústav fyziky plazmatu AV ČR, v. v. i.

*Abstrakt:* Termojaderná fúze je potenciálním zdrojem pro další staletí. K jejímu dosažení na Zemi je potřeba simulovat podmínky v centru Slunce. V takových podmínkách je veškerá hmota v plazmatickém skupenství a proto je potřeba vybudovat termojaderný reaktor, který dokáže vytvořit prostředí pro plazma. Podmínky na takový reaktor jsou stanoveny Lawsonovým kritériem. Tokamak je jedním typů termojaderných reaktorů a je mezi nimi nejbližší ke splnění tohoto kritéria. Na druhé straně bližší analýza Lawsonova kritéria stanovuje potřebu po zvětšení celého zařízení typu tokamak. Avšak velké experimenty jako ITER a DEMO jsou finančně náročné a jejich návrh a konstrukce potřebují být podloženy numerickými simulacemi. Důležitou součástí takových simulací je řešič magnetické rovnováhy.

Tato práce rozšiřuje a používá kód FREEBIE. FREEBIE je řešičem vývoje magnetické rovnováhy pro volnou hranici používaným v souboru transportních kódů, resp. projektem European Transport Solver (ETS), jehož cílem je možnost simulace celého tokamakového výboje. FREEBIE je, jakožto nedávno započatý soubor kódů, stále ve vývoji a tato práce dokumentuje jeho rozšiřování o řešič libovolných elektrických obvodů a modulem dodatečného zpracování dat. Tento řešič je potřeba k přesnějším simulacím tokamaku COMPASS. Během tohoto roku vznikla nová výzva v podobě vylepšení tokamaku COMPASS na nový, nesoucí název COMPASS-U. Tato práce přispívá do projektu COMPASS-U využitím možností kódu FREEBIE. Byla provedena studie statické magnetické rovnováhy pro různé tvary plazmatu s výsledky stanovující proudové požadavky na cívky poloidálního pole. Vertikální nestabilita byla charakterizována pro jednotlivé studované tvary dle její rychlosti růstu. Tyto výsledky jsou důležité pro návrh zdrojů tokamaku COMPASS-U a jeho zpětnovazební řízení.

*Klíčová slova:* Termojaderná fúze, Fyzika plazmatu, Tokamak, Simulace, MHD, Magnetická rovnováha

*Title:*

**Simulations of magnetic equilibrium in tokamaks**

*Author:* Martin Matušů

*Specialization:* Physics and Technology of Thermonuclear Fusion

*Work classification:* Diploma Thesis

*Supervisor:* Ing. Jakub Urban, Ph.D.  
Institute of Plasma Physics AS CR, v.v.i.

*Abstract:*

Thermonuclear fusion is a potential energy source for next few centuries. In order to control this process on Earth, it is necessary to simulate conditions of the Sun core. All matter is in plasma state in these conditions and therefore a thermonuclear reactor is needed to create an environment for the plasma. Requirements for such a reactor are stated in the Lawson criterion. The tokamak device is of all other types of thermonuclear reactor closest to fulfilment of the criterion. On the other hand, closer analysis of the Lawson criterion results in the need of scaling the tokamak device. However, large experiments like ITER and DEMO are expensive and their design and construction need to be supported by numerical simulations. An important part of such simulations is an equilibrium solver. This thesis enhances and utilizes the FREEBIE code. FREEBIE is a free-boundary equilibrium evolution solver utilized by the CRONOS transport suite or the European Transport Solver (ETS) project, whose purpose is to enable complete tokamak discharge simulations. FREEBIE is, as a recent code, still in development and this work documents effort of its enhancement by a solver of general electrical circuits and by a post-processing module. The circuit solver is particularly needed for simulations of the COMPASS tokamak. During this year, an upgrade of the COMPASS tokamak—COMPASS-U—emerged as a new, challenging project. This thesis contributes to the COMPASS-U project by exploiting the features of the FREEBIE code. Static equilibrium with various plasma shapes have been simulated, providing current requirements on the poloidal field coils. Vertical displacement events (VDE) have been characterized by their growth rates. This yields important inputs for the design of COMPASS-U power supplies and feedback systems.

*Key words:*

Thermonuclear fusion, Plasma physics, Tokamak, Simulation, MHD, Magnetic equilibrium

# Contents

|   |           |
|---|-----------|
| <b>Introduction</b>   | <b>9</b>  |
| <b>1 Thermonuclear fusion</b>                                   | <b>10</b> |
| 1.1 Principle . . . . .   | 10        |
| 1.2 Lawson criterion . . . . .                                  | 13        |
| 1.3 Tokamak . . . . .   | 16        |
| 1.3.1 Tokamak device configuration . . . . .                    | 16        |
| 1.3.2 Tokamak coordinates . . . . .                             | 17        |
| <b>2 The physics basis</b>                                      | <b>19</b> |
| 2.1 Plasma definition . . . . .                                 | 19        |
| 2.2 Particle description of plasma . . . . .                    | 22        |
| 2.2.1 The drift equation derivation . . . . .                   | 22        |
| 2.2.2 The drift equation terms and possible solutions . . . . . | 24        |
| 2.3 Magneto-Hydro dynamics . . . . .                            | 26        |
| 2.3.1 Boltzmann transport equation . . . . .                    | 26        |
| 2.3.2 Hydrodynamics and Maxwell equations . . . . .             | 27        |
| 2.3.3 Resistive and ideal MHD . . . . .                         | 29        |
| 2.4 Static equilibrium . . . . .                                | 31        |
| <b>3 Plasma simulations</b>                                     | <b>36</b> |
| 3.1 Scaling laws . . . . .                                      | 36        |
| 3.2 Integrated modelling . . . . .                              | 38        |
| 3.3 FREEBIE . . . . .   | 40        |
| <b>4 Results</b>  | <b>43</b> |
| 4.1 General electrical circuits solver . . . . .                | 43        |
| 4.2 COMPASS-U . . . . .   | 48        |
| 4.2.1 Static equilibria . . . . .                               | 48        |
| 4.2.2 Vertical Displacement Event . . . . .                     | 53        |
| 4.3 Post-processing module equi2D.py . . . . .                  | 57        |

|                     |           |
|---------------------|-----------|
| <b>Summary</b>      | <b>59</b> |
| <b>Bibliography</b> | <b>60</b> |

# Introduction

## World energy needs and nuclear power

Considering the speed of the growth of energy needs, humanity has to figure out how to solve this issue in the long term horizon. For a long time, burning fossil fuels has been a sufficient method to cover energy demands. However, this method has two problems: the fuel limitation and ecological consequences. The Manhattan project provided an alternative which was not essentially burdened by previous problems. Yet with the occurrence of accidents in fission power plants and a still growing energy demand, another source of energy is needed. With advanced knowledge of physics it may appear that renewable energy is the best way to solve this crisis. Although renewable energy may be the final solution of energetics problem of humanity, the space-efficient technology to achieve this utopia is not sufficiently developed. Therefore there is a need to find a solution in this current period. A convenient source of energy has been found by understanding the Sun. In its centre, an enormous amount of energy is generated due to the process of fusion.

# Chapter 1

## Thermonuclear fusion

### 1.1 Principle

Nuclear fusion is a process in which two or more light atomic nuclei collide to form a more complicated one. As the sum of binding energies of products is lower than sum of reactants' binding energies, their difference is released. Moreover, the difference in binding energies in fusion is much higher than in fission and such exothermic reactions are therefore potential principle of future power-plants.

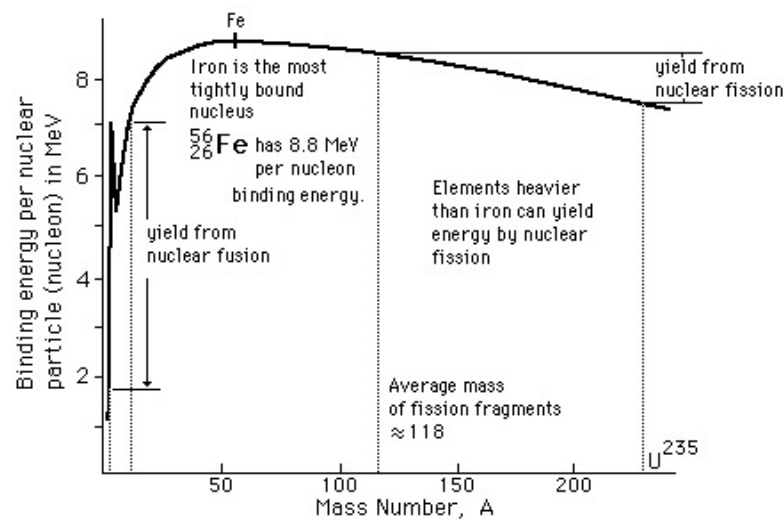
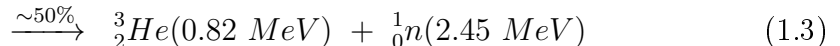


Figure 1.1: Elements stability curve visualizing fusion and fission energy yields.

In the Sun core, fusion of hydrogen nuclei (proton-proton cycle) is the main source of energy. However, the probability of its initial reactions is very small and efficient

power-plant on Earth cannot use them. On the other hand, following reactions of deuteron and tritium have largest cross-section  $\sigma^1$ , [9].



Caused by strong interaction, deuterium-tritium (D-T) reaction (1.1) is of high cross-section, i.e. probability of the reaction, and therefore the best choice of early fusion reactor principle. Although reaction of two deuterons (1.2), (1.3) is considered to precede D-T reaction in future reactors, its cross section is lower and thus undesirable as the first step.

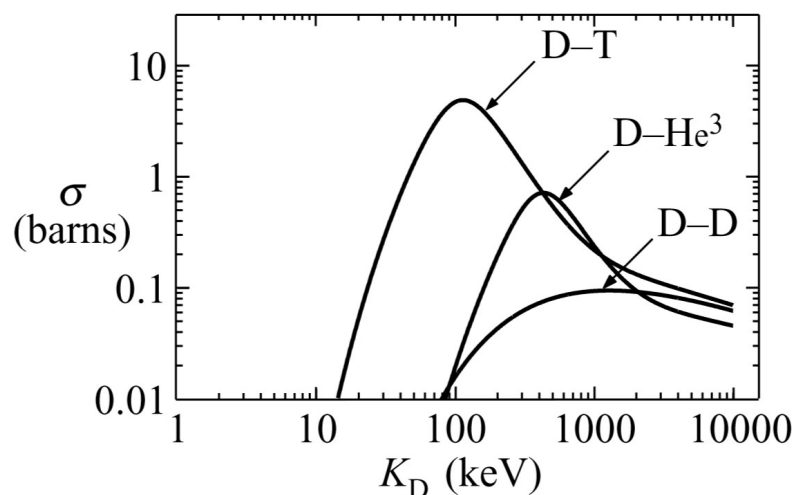


Figure 1.2: Experimental data of cross-section  $\sigma$  for D-D, D-T and D-He<sup>3</sup> reactions as a functions of deuteron energy  $K_D = m_D v_D^2/2$ ; reprinted from [9].

Considering only the reaction cross-section  $\sigma$ , according to the graph 1.2, effective reactor would need to operate at temperatures of 100 keV, i.e. about  $10^9 \text{ K}^2$ . However, in thermal equilibrium will particles energies stabilize in the form of Maxwell distribution. As the fusion reactions are considered to take place only in the hot core of the plasma, where the high energetic particles from the distribution tail are localized, lower average plasma temperatures are needed in order to generate particles with sufficient energy for

<sup>1</sup>Effective area quantifying collision likelihood.

<sup>2</sup>1 eV  $\simeq$  11600 K

the fusion process. Nevertheless, at such temperatures electrons have energies high enough to tear apart of nucleus and all matter exists in a state called plasma. Plasma definition and its characteristic behaviour is described in chapter 2.1. For now, idea of set of charged particles is sufficient.

As plasma consists of positive ions and negative electrons, it reacts to a magnetic and electric field at microscopic and macroscopic scale. As every particle is charged, bringing two ions close enough to fuse is conditioned by overcoming the electrostatic potential between them.

$$V_E = \frac{1}{4\pi\epsilon_0} \frac{Q}{r} \quad (1.4)$$

Although this force seems to grow to the infinity there exists another force, the strong interaction, which has an opposite direction, i.e. attraction. However, the strong interaction effective range is only few femtometers. This results into a finite, yet still huge potential barrier. The missing piece of the fusion puzzle was discovered by George Gamow, who explained alpha decay by quantum tunnelling. In the inverse meaning to the decay, there is a certain probability of particle tunnelling into the nucleus through the potential barrier. With knowledge of this phenomenon explaining data from observations of the Sun, the idea of controlled fusion on the Earth emerged.

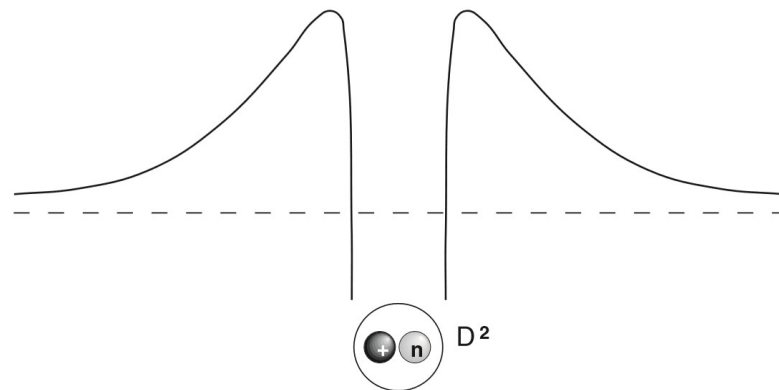


Figure 1.3: Potential barrier given by Coulomb's force and strong interaction; reprinted from [10].

## 1.2 Lawson criterion

The discussion about the fusion power-plant took place after the second world war, as the immense power hidden within an atom was demonstrated. Unfortunately, following era was burdened by informational censorship of the cold war. Therefore, international communication of scientists was limited and the research was fractured. On the other hand, variety of possible power-plant designs was invented by different countries research teams. Where United States of America developed stellarator, Soviet union came up with tokamaks. Third party in discussed research was England with its pinch research. All mentioned designs are based on the magnetic confinement of plasma. In addition, inertial confinement method was invented as laser studies were carried out.

Realizing various possibilities of approaching to the design of fusion reactor, John D. Lawson formulated in 1955 a general criterion, implying a power condition on a fusion reactor to be of a commercial usage. In the process of formulating his criterion, he introduced important variable used in tokamak physics called confinement time  $\tau_E$  as a division of plasma energy  $W_P$  and power of energy losses of plasma  $P_L$ , i.e. radiation, diffusion, etc.

$$\tau_E = \frac{W_P}{P_L} \quad (1.5)$$

Therefore, this variable maps how well confined the plasma is and how efficient would the reactor be. Power loses of plasma volume may be compensated by its heating  $P_H$ .

$$P_L = P_H - \frac{dW_P}{dt} \quad (1.6)$$

The heating may be furthermore divided into external heating  $P_e$  and heating from inner processes  $P_i$ .

$$P_H = P_e + P_i \quad (1.7)$$

Heating by inner processes is equivalent of the power of the fusion reaction captured in the plasma. In the special case of the D-T fusion(1.1) alpha particles, achieving one fifth of the fusion energy  $P_f$  thanks to the third of Newton's laws of motion, are captured in plasma. The rest of the energy is taken away by neutrons captured in the reactor and its thermal energy is the outcome of the reactor further transformed into electricity.

$$P_i = \frac{1}{5}P_f \quad (1.8)$$

Fusion power  $P_f$  is of course dependent on the volume of the plasma  $V_p$ , energy gain of one reaction  $\varepsilon_f$  and the rate of fusion reactions in this volume  $R_V$ . This rate is a multiplication of fuel densities  $n_{f1}, n_{f2}$  and reactivity, i.e. average of the cross section and relative velocity  $\langle \sigma v_r \rangle$ .

$$P_f = R_V V_p \varepsilon_f = n_{f1} n_{f2} \langle \sigma v_r \rangle V_p \varepsilon_f. \quad (1.9)$$

Plasma energy in the initial equation (1.5) may be rewritten as well. Considering the equipartition theorem for monoatomic nonideal gas

$$W_P = \int_{V_P} 3(n_{f1} + n_{f2})k_B T dV_P = 3k_B \overline{(n_{f1} + n_{f2})} TV_p \quad (1.10)$$

and additional condition of flat profiles of densities and temperature, confinement time (1.5) may be rewritten by (1.6-1.10) as follows

$$\begin{aligned} \tau_E &= \frac{W_P}{P_e + P_f - \frac{dW_P}{dt}} \\ \tau_E &= \frac{3k_B(n_{f1} + n_{f2})TV_p}{P_e + \frac{1}{5}n_{f1}n_{f2} \langle \sigma v_r \rangle V_p \varepsilon_f - \frac{d(3(n_{f1} + n_{f2})k_B TV)}{dt}} \\ P_e + \frac{1}{5}n_{f1}n_{f2} \langle \sigma v_r \rangle V_p \varepsilon_f &= \frac{3k_B(n_{f1} + n_{f2})TV_p}{\tau_E} + \frac{d(3(n_{f1} + n_{f2})k_B TV)}{dt} \\ P_e + \frac{1}{20}n^2 \langle \sigma v_r \rangle V_p \varepsilon_f &= \frac{3k_B n TV_p}{\tau_E} + \frac{d(3nk_B TV)}{dt} \end{aligned} \quad (1.11)$$

The last equation is a special case of D-T fusion, when fuel densities are equal, i.e.  $n_D = n_T = \frac{n}{2}$ . As mentioned above, the Lawson criterion discuss a commercial power-plant. Hence, heating of the plasma by fusion itself demand is reasonable. In such state, the external heating power  $P_e$  diminish. In the extremal state of power equilibrium, plasma energy would be constant and the derivative in 1.11 would diminish as well. This extremal state is called ignition and sets the minimal value of the right hand side (RHS) of the equation. The Lawson criterion itself is in the form of inequality for the confinement time

$$\tau_E \geq \frac{W_P}{P_H} = \frac{60k_B T}{n \langle \sigma v_r \rangle \varepsilon_f} \quad (1.12)$$

A more useful way of formulating the criterion is to substitute all temperature dependent variables as a single function  $f_L(T)$ .

$$\tau_E n \geq f_L(T). \quad (1.13)$$

For the D-T reaction, this function reaches its minimum at the temperature  $T = 30$  keV, [20, p.90].

### Triple product

However, plasma density is function of temperature as well. In the special case of the magnetic confined fusion is the plasma pressure given by magnetic field and its dependency upon temperature is negligible. Under the approximation of plasma as ideal gas its density is inversely proportional to the temperature. Therefore, the dependency of confinement time upon temperature becomes quadratic.

$$\tau_E \sim \frac{T^2}{\langle \sigma v_r \rangle} \quad (1.14)$$

Under such conditions, ideal temperature shifts to  $T = 10-20$  keV, where  $\tau_E$  has minimum. As this minimum is relatively flat, reactivity may be considered as quadratically dependent on temperature in this area  $\langle \sigma v_r \rangle \sim T^2$ . By substituting this fact in Lawson criterion (1.12) and enumerating all constants, triple product for D-T fusion in magnetic confined plasma is obtained.

$$n\tau_E T \geq 3 \times 10^{21} \text{ m}^{-3} \text{ keVs} \quad (1.15)$$

## 1.3 Tokamak

Nowadays, tokamaks have a prime role in the fusion research. Taking into account designs mentioned above, i.e. tokamak, stellarator, pinch and inertial fusion, the elimination process leaves tokamaks as least problematic and closest to the fusion power-plant. Inertial fusion considers as a drive for plasma heating lasers, yet laser technology is not advanced enough to supply the drive often enough for effective power plant. The cost of multiplying lasers would set an immense financial offset for the device. Magnetic confined designs are closer to a fulfilment of Lawson criterion. However, the thermonuclear z-pinch design is based on self-destruction and its possibility of continuous energy production desired by a power-plant is scant. Moreover, its confinement times are far behind stellarators and tokamaks. On the other hand, densities in z-pinch experiments are exceptional, which makes this design unique tool of plasma studies. Stellarators are precisely designed devices with no invoked plasma current. Therefore, current disruptions and other events caused by plasma current are not present. On the other hand, stellarator twisted coils are immensely strained by asymmetric forces caused by magnetic field and thus limitations of plasma confinement is present. As tokamak design has complex plasma conditions, e.g. inhomogeneous magnetic field, tokamak physics emerged as a new branch. In order to describe tokamak physics, the device and its coordinates description is necessary.

### 1.3.1 Tokamak device configuration

The path of a charged particle in magnetic field is twisted by Lorentz force and if the velocity of the particle is not perpendicular to the magnetic field, the resulting trajectory is of helical shape, i.e. without external disruptions particle follows a magnetic field line. Hence, tokamaks enclose magnetic field in toroidal shape in order to maintain the plasma during an experiment and thus the plasma shapes itself similarly with the vacuum vessel enclosing it. Furthermore, this configuration is axis-symmetric<sup>3</sup>, which simplifies tokamak physics and is one of advantages against stellarators. The axis-symmetry is approximate as coils creating the field are not continuous, resulting in a ripple between those coils.

In order to achieve the described configuration, tokamak device itself consists of few basic structures: the vacuum vessel of a toroidal shape and toroidal field coils. Current in toroidal field coils is the source of the toroidal magnetic field  $B_t$  and toroidal field coils surround vessel in poloidal direction<sup>4</sup>. Moreover, a set of poloidal field coils is necessary in tokamak device, as described in chapter 2.2. These coils influence poloidal magnetic field  $B_p$  and their geometry is therefore in the toroidal direction<sup>5</sup>, i.e. parallel to the vessel.

---

<sup>3</sup>Tokamak physics is therefore often labelled to take place in 2.5 dimensional space.

<sup>4</sup>Perpendicular to the toroidal direction, around the vessel cross-section.

<sup>5</sup>The designation of coils is sometimes commuted in technical descriptions of the device; this work uses modern tokamak physics convention.

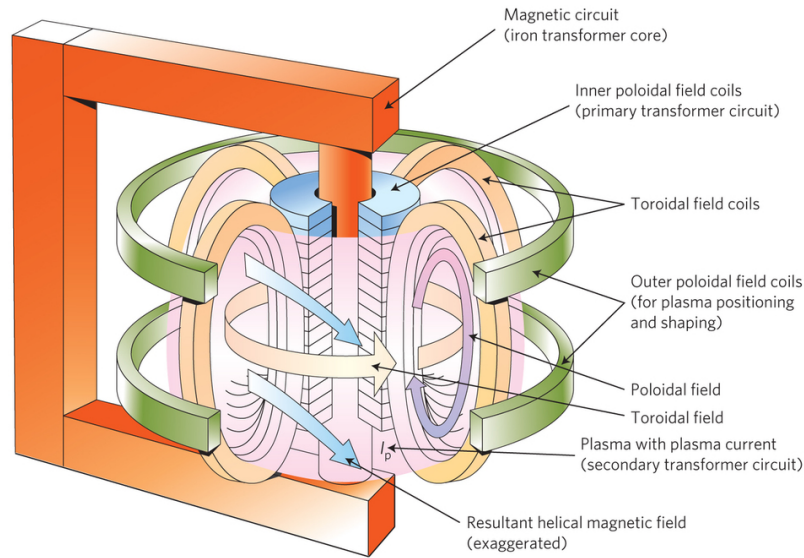


Figure 1.4: Illustration of basic structures of the tokamak device and magnetic field in the vacuum vessel; reprinted from [11].

The last basic component a tokamak device is supplemented by are transformer windings. Using plasma as secondary winding, these windings are used to generate plasma current  $I_p$  flowing in toroidal direction, which in turn create strong poloidal magnetic field  $B_p$ . The transformers in modern tokamaks mostly use air core and some of older tokamaks still use an iron core illustrated in figure 1.4. Although poloidal magnetic field is mandatory for tokamak physics, there are other ways to generate plasma current, e.g. current driven by neutral beam injection. On the contrary, due to its derivative character, plasma current driven only by transformer principle is undesired and therefore studies supporting other ways of a current drive are undergone. As most components in tokamak are curved in toroidal or poloidal direction, Cartesian coordinate system is usually inconvenient for the description and different coordinate systems need to be introduced.

### 1.3.2 Tokamak coordinates

In order to emphasize the axis-symmetry of tokamak, description by cylindrical coordinates  $(R, \varphi, Z)$  is often of use. The radius  $R$  is a coordinate measuring the distance from symmetry axis,  $\varphi$  designates the toroidal angle and  $Z$  is classic Cartesian coordinate  $(x, y, z)$  situated in the direction of the symmetry axis. By convention, coordinate system origin is placed at the symmetry axis and in the half of the height of the tokamak. Transformations from Cartesian coordinate system may be denoted as

$$\begin{aligned} R^2 &= x^2 + y^2, \\ \tan\phi &= \frac{y}{x}. \end{aligned} \tag{1.16}$$

Another transformation results in simple toroidal coordinates  $(r, \phi, \vartheta)$ . This coordinate system description is mostly used for description of in-vessel phenomena and structures. In this coordinate system,  $r$  describes length from axis of a torus, which has constant distance  $R_0$  from symmetry axis called major radius. In order to describe in-vessel components only,  $r$  is limited  $0 < r < a$ , where  $a$  denotes minor radius. The remaining coordinates are toroidal angle  $\phi$  as in cylindrical coordinates and poloidal angle  $\vartheta$  between radius  $r$  and equatorial plane, i.e. plane perpendicular to symmetry axis containing axis of the torus, beginning at the outer part of torus. Transformation set of equations between simple toroidal coordinates and cylindrical coordinates is denoted as

$$\begin{aligned} R &= R_0 + r\cos\theta, \\ Z &= r\sin\theta. \end{aligned} \tag{1.17}$$

Both coordinate systems are illustrated at 1.5. In further text will be cylindrical coordinates used the most.

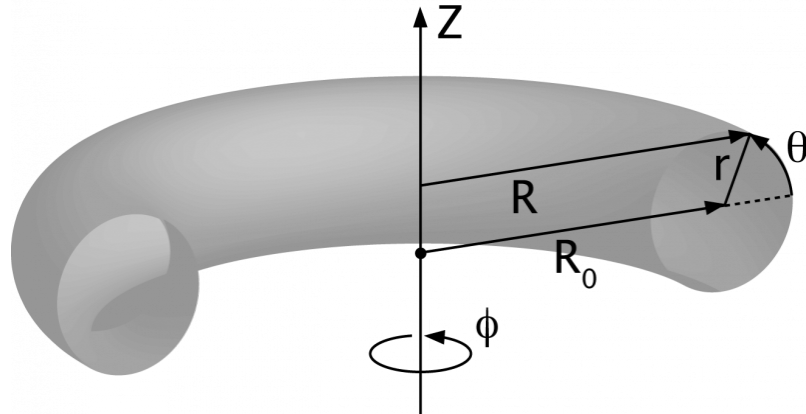


Figure 1.5: Illustration of cylindrical and simple toroidal coordinate systems used for tokamak description; reprinted from [23].

# Chapter 2

## The physics basis

At temperatures  $10 - 20 \text{ keV}$  discussed in chapter (1.2), all matter is in the plasma, so called fourth state. Hence, plasma definition is required for further physics derivation.

### 2.1 Plasma definition

“Plasma is a quasi-neutral gas of charged and neutral particles, which shows collective behaviour.”

-Francis F. Chen, [5, p.19]

Looking closer at this definition, there are two important points: quasi-neutrality and collective behaviour. The meaning of this expression is in more detail described and rewritten in following three conditions:

1. Plasma range

Because the particles in plasma are charged, any segregation of electrons from ions converts their kinetic energy into electrostatic potential. This depends on density  $n_e$  of displaced electrons and the volume of displaced electrons, specially in the 2D approximation width  $\Delta$  of the electron layer. The maximum width, when the layer is displaced by its own width and all kinetic energy  $E_k$  is converted into the potential  $U_p = -eE\Delta$  because of this displacement, is named the Debye length  $\lambda_D$ . While kinetic energy may be expanded as a product of Boltzmann's constant  $k_B$  and the electron temperature  $T_e$ , the potential energy is an integral of the electric force  $eE$  over the distance  $\lambda_D$ . By consideration of the displaced layer as a 2D capacitor of thickness  $\lambda_D$ , the electric field  $E$  fulfils equation

$$E = -en_e\lambda_D/\epsilon_0. \tag{2.1}$$

Summing up, the equality of these energies concludes in definition

$$max \Delta = \lambda_D = \left( \frac{\epsilon_0 k_B T_e}{n_e e^2} \right)^{\frac{1}{2}}. \quad (2.2)$$

This length is used in the description of quasi-neutrality. It is the distance, at which the charges in the plasma remains unshielded by other charges. Therefore the whole plasma is neutral, but within a sphere around the charge with this radius, Coulomb force is essential. The first condition of plasma has to be therefore set, so that Debye length has to be much smaller than system size:  $L \gg \lambda_D$ .

## 2. Dominance of EM force

The quasi-neutrality term is not valid with quick processes because of the short duration of the mentioned dislocation. In the case of the capacitor described above, dislocation of negative charge with respect to positive background initiates harmonic oscillations with the plasma frequency  $\omega_{pe}$ . It is possible to describe this electron displacement  $\Delta$  as an equation of motion, where electrons with the mass  $m_e$  and the charge density  $en_e$  experience a restoring force  $eE$  created by the electric field (2.1)<sup>1</sup>,

$$m_e \frac{d^2 \Delta}{dt^2} = - \frac{e^2 n_e}{\epsilon_0} \Delta, \quad (2.3)$$

where  $\epsilon_0$  is the vacuum permittivity. (2.3) is an equation of a harmonic oscillator with a characteristic frequency

$$\omega_{pe} = \left( \frac{n_e e^2}{\epsilon_0 m_e} \right)^{\frac{1}{2}}. \quad (2.4)$$

This variable is called the characteristic plasma oscillation frequency. In order to call a ionised gas a plasma, the electromagnetic force has to be dominant over collisions with neutral particles. If the average time between these collisions is  $\tau_{col}$ , there has to be fulfilled the condition  $\tau_{col} \omega_{pe} > 1$ . This condition describes whether a gas acts as plasma or as a neutral gas, [5, p.26].

## 3. Plasma parameter

To further describe plasma in which collective behaviour dominates binary collision it is necessary to realize, that distant particles affect charged particle much less in comparison with adjacent ones. This phenomenon is called Debye shielding and

---

<sup>1</sup> $\lambda_D$  describes maximal value of displacement and is therefore replaced by width  $\Delta$

considers  $\lambda_D$  great enough to contain a lot of particles in its sphere independently of electron density. This condition is formulated by plasma parameter

$$N_D = \frac{4\pi}{3}\lambda_D^3 n_e \gg 1. \quad (2.5)$$

Because this definition is quite general, plasma may occur in different forms. Its density may differ by thirty orders of magnitude and temperature by ten orders of magnitude (see figure 2.1). From this figure should be pointed out Sun's core, whose principle have scientists tried to explain for many centuries, and Tokamaks with Inertial confined fusion (ICF), methods to simulate equivalent conditions on Earth, already standing just next to it.

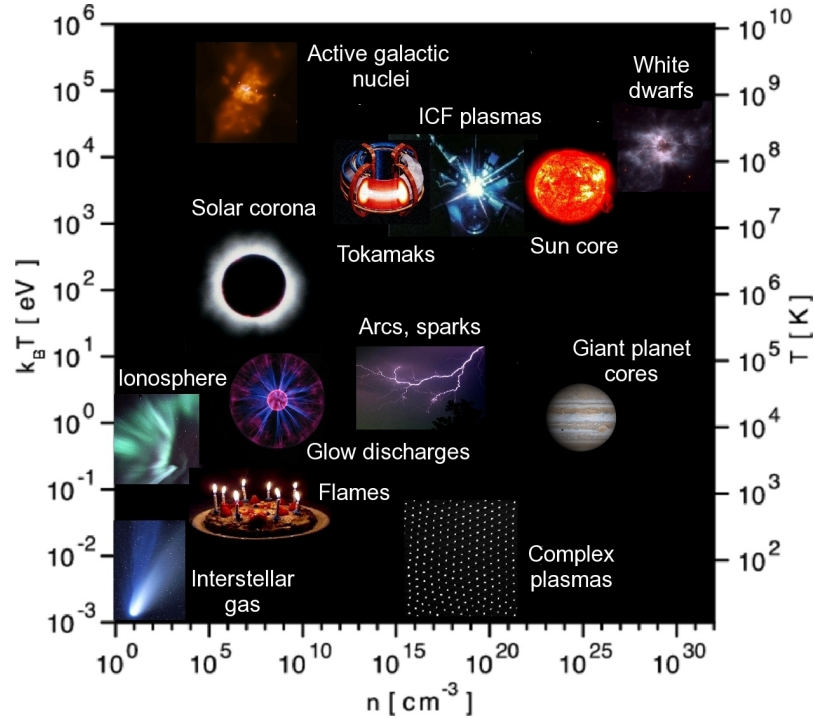


Figure 2.1: Forms of plasma:  $n$  stands for density,  $E = k_B T$  is energy and  $T$  its temperature equivalent; reprinted from [22].

## 2.2 Particle description of plasma

Although plasma reacts to electro-magnetic(EM) field with collective behaviour, keystones of understanding many physics phenomena are description of its elementary processes and addition of discrete elementary results into more complex model. Study of particles in electro-magnetic field follows this approach. The movement of a single particle in electro-magnetic field is given by Lorentz force

$$\mathbf{F}_L = q(\mathbf{E} + \mathbf{v} \times \mathbf{B}), \quad (2.6)$$

where  $q$  stands for a charge of a particle,  $\mathbf{v}$  is its velocity and  $\mathbf{E}$  with  $\mathbf{B}$  are electric and magnetic field respectively. Under various conditions the resulting complexity of a particle trajectory varies. For example in homogeneous  $B$  and negligible  $E$  particle trajectory is a helix given by a set of equations,

$$\begin{aligned} \ddot{x} &= \frac{QB}{m} \dot{y} \quad \equiv \omega_c \dot{y}, \\ \ddot{y} &= -\frac{QB}{m} \dot{x} \quad \equiv \omega_c \dot{x}, \end{aligned} \quad (2.7)$$

where  $\omega_c$  is cyclotron frequency and the movement is visualized in the figure 2.2. Similarly in more complicated configurations, because of the vector multiplication in the formula (2.6), the particle will always orbit around the so called centre of a gyration and the resulting movement is a superposition of orbit movement and movement of the guiding centre.

### 2.2.1 The drift equation derivation

Specific variables as radius of the gyration, i.e. orbiting movement, might be derived, yet for further description a precise knowledge of particle movement is unnecessary and the problem may be reduced on study of the gyration centre movement. This is achieved by calculation of an average of the movement equation

$$m\ddot{\mathbf{r}} = \mathbf{F}_{ext}(t, \mathbf{r}) + q\dot{\mathbf{r}} \times \mathbf{B}(t, \mathbf{r}), \quad (2.8)$$

over the gyration movement. In equation (2.8), the electric component of the Lorentz force is generalized into  $\mathbf{F}_{ext}$  including any external forces as gravitational one. The average is made under a condition of minor changes to EM field experienced by the particle during the gyration. The resulting equation for the guiding centre

$$\begin{aligned} m\ddot{\mathbf{R}} &= \mathbf{F}_{ext} + q\dot{\mathbf{R}} \times \mathbf{B} - \mu\nabla B, \\ \mu &= \frac{mv_{\perp}^2}{2B}, \end{aligned} \quad (2.9)$$

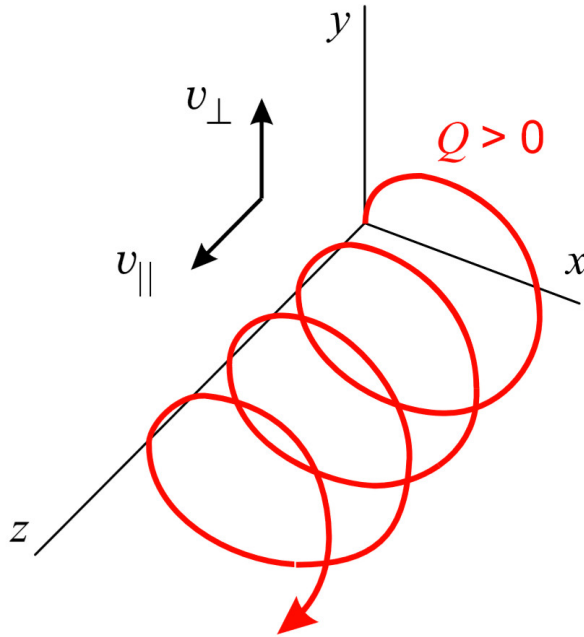


Figure 2.2: Visualisation of the gyration of ion in the magnetic field alongside the z-axis, thus designation  $v_{\parallel}$  for velocity component parallel to the magnetic field and the perpendicular one  $v_{\perp}$ ; reprinted from [18].

where particle location  $\mathbf{r}$  vanishes from the equation due the process of averaging and description of the guiding centre position  $\mathbf{R}$  remains<sup>2</sup>. In the last term of the equation was used designation  $\mu$  called first adiabatic invariant and its meaning is discussed in [18]. The equation introduces a force  $-\mu\nabla B$  which influence lies in the guiding centre and pushes the particle out of strong fields. The configuration in tokamak is influenced by this force as toroidal magnetic field  $B_{\phi}$  is stronger near the axis in comparison to the further side of the chamber. Such field inhomogeneity is a result of the toroidal configuration and leads to often used description of the chamber sides as High Field Side (HFS) and Low Field Side (LFS). In order to conduct further examination of guiding center movement in non-trivial EM field, it is convenient to perform cross multiplication of the guiding centre movement equation by magnetic field  $B$ . The double vector product identity application at the second term on the Right Hand Side (RHS) of the equation yields with minor adjustments

---

<sup>2</sup>Precise derivation is done by position vector decomposition  $\mathbf{r}(t, \tau) = \mathbf{R}(t) + \epsilon\rho(t, \tau)$ , where  $\rho$  stands for relative position of the particle and the guiding centre and  $\epsilon \rightarrow 1$  after the averaging over fast time of the gyration  $\tau$ .

$$\dot{\mathbf{R}} - \left( \dot{\mathbf{R}} \cdot \frac{\mathbf{B}}{B} \right) \frac{\mathbf{B}}{B} = \frac{\mathbf{F}_{ext} \times \mathbf{B} - \mu \nabla B \times \mathbf{B} - m \ddot{\mathbf{R}} \times \mathbf{B}}{QB^2}. \quad (2.10)$$

Finally, by realization what that second term of the LHS is a projection of guiding centre velocity  $\dot{\mathbf{R}}$  into the direction of magnetic field. Therefore, whole LHS might be labelled as  $\dot{R}_\perp$ , i.e. component of guiding centre velocity perpendicular to the magnetic field

$$\dot{\mathbf{R}}_\perp = \frac{\mathbf{F}_{ext} \times \mathbf{B} - \mu \nabla B \times \mathbf{B} - m \ddot{\mathbf{R}} \times \mathbf{B}}{QB^2}. \quad (2.11)$$

This equation is called the drift equation as it describes how particles escapes the confinement and pass across the magnetic field lines.

### 2.2.2 The drift equation terms and possible solutions

The drift equation (2.11) RHS consist of three terms, each describing different type of drift.

The first term describes drift of a particle due to an external force  $\mathbf{F}_{ext}$ . Particularly for electric component of Lorentz force  $\mathbf{F}_{ext} = q\mathbf{E}$  a drift independent of particle charge is obtained

$$\mathbf{v}_E = \frac{\mathbf{E} \times \mathbf{B}}{B^2} \quad (2.12)$$

The resulting drift will be perpendicular to both electric and magnetic field, thus it is labelled as  $\mathbf{E} \times \mathbf{B}$  drift. Another force influencing plasma particles is gravitational force  $\mathbf{F}_{ext} = m\mathbf{g}$ .

$$\mathbf{v}_g = \frac{m\mathbf{g} \times \mathbf{B}}{qB^2} \quad (2.13)$$

On the contrary to  $\mathbf{E} \times \mathbf{B}$  drift, gravitational one is dependant on particle charge  $q$  and mass  $m$ . This will result in separation of ions and electrons. Thus, electric field  $\mathbf{E}$  is created, leading to  $\mathbf{E} \times \mathbf{B}$  drift. The second term describes so called grad B drift mentioned earlier.

$$\mathbf{v}_{\nabla B} = \frac{-\mu \nabla B \times \mathbf{B}}{qB^2} = \frac{mv_\perp^2}{2q} \frac{\nabla B \times \mathbf{B}}{B^3} \quad (2.14)$$

Thanks to the cross product with magnetic field  $\mathbf{B}$  itself, the resulting drift is not directly outwards of the stronger magnetic field, yet it is dependant on magnitude of magnetic field. Moreover, similarly to gravitational drift, grad B drift is dependant on

particle charge  $q$  and mass  $m$  and thus leads to charge separation followed by  $\mathbf{E} \times \mathbf{B}$  drift as well.

At last, the third term is dependant on the shape of magnetic field and is called the curvature drift. It may be understood similarly as the first term, only with force caused by particle motion and not external.

$$\mathbf{F} = m\ddot{\mathbf{R}} = \frac{mv_{\parallel}^2}{R_k} \frac{\mathbf{R}_k}{R_k} \quad (2.15)$$

As the movement of the guiding centre of a particle is basically given by a magnetic field line, its curvature will result in a centrifugal force mentioned in (2.15), where  $\mathbf{R}_k$  stands for radius of field line curvature. The resulting drift velocity

$$\dot{\mathbf{r}}_{\mathbf{R}} = \frac{mv_{\parallel}^2}{qB^2} \frac{\mathbf{R}_k \times \mathbf{B}}{R_k^2}, \quad (2.16)$$

which is dependant on particle charge  $q$  and mass  $m$  again, leading to  $\mathbf{E} \times \mathbf{B}$  drift.

All discussed drifts dependant on particle charge  $q$  are present in toroidal configuration and lead to  $z_+$  vs.  $z_-$  charge separation. Resulting electric field is therefore along  $z$  axis and  $\mathbf{E} \times \mathbf{B}$  drift direction is towards LFS (visualized in figure 2.3).

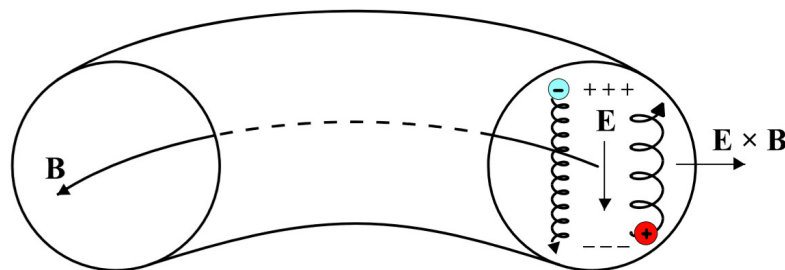


Figure 2.3: Separation of ions and electrons leading to vertical electric field  $\mathbf{E}$  resulting in  $\mathbf{E} \times \mathbf{B}$  drift; reprinted from [18].

This phenomenon is a problem of both tokamaks and stellarators and the solution in each is to let particles pass periodically through LFS and HFS, i.e. helical movement of charged particles. However, the realization differs between mentioned configurations. Stellarators give up on toroidal symmetry and change the geometry of external coils, causing poloidal component of magnetic field  $B_{\theta}$  to appear. In the contrary, tokamaks choose to keep the axis-symmetry and create the poloidal component by driving current through plasma column.

## 2.3 Magneto-Hydro dynamics

Although particle description approach used in chapter 2.2 is useful especially in diffusion calculations, number of particles in tokamak is in order of  $10^{18} m^{-3}$  and it would be hardly used to describe them all. However it is possible to describe all particles as a statistical ensemble and further approximate the system by describing the plasma as continuous matter. This description approaches plasma as a conducting liquid. Under specific conditions, described in the process later, Those equations may be combined with the set of Maxwell equations and result in Magneto-Hydro Dynamics (MHD) set of equations.

### 2.3.1 Boltzmann transport equation

Particle description of a system is provided by its probability density function  $f_\alpha(t, \mathbf{x}, \mathbf{v}_\alpha)$  of  $\alpha$ -species particle. This equation is a function of seven variables and is normed by number of particles  $N_\alpha$  and its density  $n_\alpha$ , i.e.

$$\begin{aligned} \int f_\alpha(t, \mathbf{x}, \mathbf{v}_\alpha) d^3 \mathbf{v}_\alpha &= n_\alpha(t, \mathbf{x}), \\ \int f_\alpha(t, \mathbf{x}, \mathbf{v}_\alpha) d^3 \mathbf{x} d^3 \mathbf{v}_\alpha &= N_\alpha(t). \end{aligned} \quad (2.17)$$

The particle probability function vary due to collisions between particles of the same species  $\alpha$  and with any other species  $\beta$

$$\frac{d}{dt} f_\alpha(t, \mathbf{x}, \mathbf{v}_\alpha) = \sum_{\beta} S_{\alpha\beta}, \quad (2.18)$$

where  $S_{\alpha\beta}$  is a general collisional term of species  $\alpha$  and  $\beta$ . By expanding the LHS according to chain rule and expressing time derivations of location as velocity  $v_{k\alpha}$  and acceleration

$$\frac{\partial f_\alpha}{\partial t} + v_{k\alpha} \frac{\partial f_\alpha}{\partial x_k} + \frac{F_{k\alpha}}{m_\alpha} \frac{\partial f_\alpha}{\partial v_{k\alpha}} = \sum_{\beta} S_{\alpha\beta}, \quad k \in 1, 2, 3, \quad (2.19)$$

where the summation at LHS might be rephrased as operators and desired Boltzmann equation

$$\frac{\partial f_\alpha}{\partial t} + (\mathbf{v}_\alpha \cdot \nabla_{\mathbf{x}}) f_\alpha + \frac{1}{m_\alpha} (\mathbf{F}_\alpha \cdot \nabla_{\mathbf{v}}) f_\alpha = \sum_{\beta} S_{\alpha\beta}, \quad (2.20)$$

which is basic equation for statistics of nonequilibrium systems. More precise derivation with discussed assumptions may be found in [10]. Moreover, let there be a summation

invariant  $\Phi$  of a collision, i.e. variable which overall value of all actors before and after the collision does not change only distributes between actors<sup>3</sup>

$$\Phi_\alpha + \Phi_\beta = \Phi'_\alpha + \Phi'_\beta. \quad (2.21)$$

For such summation invariant is valid a relation

$$\sum_{\alpha,\beta} \int \Phi_\alpha S_{\alpha\beta} d^3\mathbf{v}_\alpha = 0, \quad (2.22)$$

proved in [18] as well. This information might be quite well used in so called momentum equation derived by multiplying Boltzmann equation (2.20) by  $\Phi_\alpha(\mathbf{v}_\alpha)$  and integrating it over velocity space. Important relation used in the derivation is average of arbitrary variable  $V$

$$\langle V \rangle_{\mathbf{v}} = \frac{\int V f_\alpha(t, \mathbf{x}, \mathbf{v}_\alpha) d^3\mathbf{v}_\alpha}{\int f_\alpha(t, \mathbf{x}, \mathbf{v}_\alpha) d^3\mathbf{v}_\alpha}. \quad (2.23)$$

Momentum equation is a basic transport equation for the continuum theory and is of form

$$\frac{\partial}{\partial t} \langle n_\alpha \Phi_\alpha \rangle_{\mathbf{v}} + \nabla_{\mathbf{x}} \cdot \langle n_\alpha \Phi_\alpha \mathbf{v}_\alpha \rangle_{\mathbf{v}} - \frac{q_\alpha}{m_\alpha} \left\langle n_\alpha (\mathbf{E} + \mathbf{v}_\alpha \times \mathbf{B}) \cdot \frac{\partial \Phi_\alpha}{\partial \mathbf{v}_\alpha} \right\rangle_{\mathbf{v}} = \int \Phi_\alpha \sum_{\beta} S_{\alpha\beta} d^3\mathbf{v}_\alpha. \quad (2.24)$$

### 2.3.2 Hydrodynamics and Maxwell equations

Specification of the summation invariant in the momentum equation (2.24) results in various equations. For the null moment a constant is taken  $\Phi = 1$ . Although charge  $q_\alpha$  and mass  $m_\alpha$  of a particle yields similar results, these are not of further use in this derivation. The moment equation takes form of continuity equation for particles of species  $\alpha$

$$\frac{\partial n_\alpha}{\partial t} + \nabla \cdot (n_\alpha \mathbf{u}_\alpha) = 0 \quad (2.25)$$

meaning that particles are conserved within the system. Similarly collisional invariant is momentum of particles  $\Phi = m_\alpha \mathbf{v}_\alpha$  and energy  $\Phi = \frac{1}{2} m_\alpha \mathbf{v}_\alpha^2$  leading to 1<sup>th</sup> component of particle momentum equation and energy equation respectively

---

<sup>3</sup>Few examples for insight: mass, charge, momentum, energy

$$\frac{\partial}{\partial t} (n_\alpha m_\alpha u_{\alpha l}) + \frac{\partial}{\partial x_k} (n_\alpha m_\alpha \langle v_{\alpha k} v_{\alpha l} \rangle_{\mathbf{v}}) - n_\alpha q_\alpha (\mathbf{E} + \mathbf{u}_\alpha \times \mathbf{B})_l = \int m_\alpha v_{\alpha l} \sum_\beta S_{\alpha\beta} d^3 \mathbf{v}_\alpha, \quad (2.26)$$

$$\frac{\partial}{\partial t} \left( \frac{1}{2} n_\alpha m_\alpha \langle v_\alpha^2 \rangle_{\mathbf{v}} \right) + \nabla_{\mathbf{x}} \cdot \left( \frac{1}{2} n_\alpha m_\alpha \langle v_\alpha^2 \mathbf{v}_\alpha \rangle_{\mathbf{v}} \right) - n_\alpha q_\alpha \mathbf{E} \cdot \mathbf{u}_\alpha = \int \frac{1}{2} m_\alpha v_\alpha^2 \sum_\beta S_{\alpha\beta} d^3 \mathbf{v}_\alpha. \quad (2.27)$$

In the equations were introduced term of average velocity for particle species  $\mathbf{u}_\alpha$  which in addition to chaotic, i.e. thermal, component  $\mathbf{w}_\alpha$  describe original velocity  $\mathbf{v}_\alpha$ .

$$\mathbf{w}_\alpha = \mathbf{v}_\alpha - \mathbf{u}_\alpha \quad (2.28)$$

By substitution of relation (2.28) into momentum and energy equation (2.26),(2.27) and introduction of thermal quantities

$$\begin{aligned} \rho_\alpha &\equiv n_\alpha m_\alpha && (\text{mass density}), \\ \rho_{q,\alpha} &\equiv q_\alpha m_\alpha && (\text{charge density}), \\ T_\alpha(t, \mathbf{r}) &\equiv \frac{m_\alpha}{3k} \langle w_\alpha^2 \rangle && (\text{temperature}), \\ \overleftrightarrow{\mathbf{P}}_\alpha(t, \mathbf{r}) &\equiv \rho_\alpha \langle \mathbf{w}_\alpha \cdot \mathbf{w}_\alpha \rangle = p_\alpha \overleftrightarrow{\mathbf{I}} + \overleftrightarrow{\boldsymbol{\pi}}_\alpha && (\text{stress tensor}), \\ \mathbf{h}_\alpha(t, \mathbf{r}) &\equiv \frac{1}{2} \rho_\alpha \langle w_\alpha^2 \mathbf{w}_\alpha \rangle && (\text{heat flow}), \\ \mathbf{R}_\alpha(t, \mathbf{r}) &\equiv m_\alpha \int \mathbf{v}_\alpha \sum_\beta S_{\alpha\beta} d^3 \mathbf{v}_\alpha && (\text{momentum transfer}), \\ Q_\alpha(t, \mathbf{r}) &\equiv \frac{1}{2} m_\alpha \int v_\alpha^2 \sum_\beta S_{\alpha\beta} d^3 \mathbf{v}_\alpha && (\text{heat transfer}), \end{aligned} \quad (2.29)$$

where  $k$  stands for the Boltzmann constant, the resulting set in addition to continuity equation (2.25) takes form

$$\begin{aligned} \frac{\partial n_\alpha}{\partial t} + \nabla \cdot (n_\alpha \mathbf{u}_\alpha) &= 0, \\ \rho_\alpha \left( \frac{\partial \mathbf{u}_\alpha}{\partial t} + \mathbf{u}_\alpha \cdot \nabla \mathbf{u}_\alpha \right) + \nabla \cdot \mathbf{P}_\alpha - \rho_{q,\alpha} (\mathbf{E} + \mathbf{u}_\alpha \times \mathbf{B}) &= \mathbf{R}_\alpha, \\ \frac{3}{2} n_\alpha k \left( \frac{\partial T_\alpha}{\partial t} + \mathbf{u}_\alpha \cdot \nabla T_\alpha \right) + \mathbf{P}_\alpha : \nabla \mathbf{u}_\alpha + \nabla \cdot \mathbf{h}_\alpha &= Q_\alpha. \end{aligned} \quad (2.30)$$

which is still open. One of possible closures is the polytrope equation

$$\frac{d}{dt} (p_\alpha \rho_\alpha^{-\gamma}) = 0. \quad (2.31)$$

### 2.3.3 Resistive and ideal MHD

As plasma consist of separated ions and electrons of different mass  $m_e, m_i$  and charges  $q_e = -e, q_i = Ze$ , where  $e$  stands for elementary charge and  $Z$  is average charge state, two-fluid description would be adequate for plasma description. However, for the binding between ions and electrons as they origin from the same neutrals, generalization for one-fluid equations may be done by introduction of macroscopic quantities

$$\begin{aligned}
 \rho &\equiv n_e m_e + n_i m_i && \text{(total mass density),} \\
 \rho_q &\equiv -e(n_e - Zn_i) && \text{(charge density),} \\
 \mathbf{v} &\equiv (n_e m_e \mathbf{u}_e + n_i m_i \mathbf{u}_i) / \rho && \text{(centre of mass velocity),} \\
 \mathbf{j} &\equiv -e(n_e \mathbf{u}_e + Zn_i \mathbf{u}_i) && \text{(current density),} \\
 p &\equiv p_e + p_i && \text{(pressure).}
 \end{aligned} \tag{2.32}$$

Equations (2.32) need to be inverted in order to rephrase hydrodynamic equations (2.30). Moreover, following approximations simplify the inversion and allow the formulation of so called resistive MHD equations.

- $|\mathbf{u}_i - \mathbf{u}_e| \ll v$ , where  $v$  stands for typical velocities of described phenomena by the model. Although electrons' velocity is higher, average component of velocity is discussed for  $\mathbf{u}_\alpha$ , this approximation of small relative velocities is satisfied.
- $|n_e - Zn_i| \ll n_e$  discuss charge distribution and is satisfied in plasmas thanks to its quasi neutrality behaviour described in chapter (2.1).
- $\tau_{MHD} \sim a/v_A \gg \omega_i^{-1}$  is a limitation of time-scale of described phenomena. In the approximation time scale of described events  $\tau_{MHD}$  is similar to the time of passing plasma dimension  $a$  by phenomena, e.g. wave, by Alfvén velocity  $v_A$ , which is a characteristic quantity for plasma. At last,  $\omega_i^{-1}$  stands for ion cyclotron frequency. The limitation therefore cuts off high frequency phenomena spectrum.
- By approximation of  $\overleftrightarrow{\pi}_{e,i} \sim \overleftrightarrow{0}$ ,  $\mathbf{h}_{e,i} \sim \mathbf{0}$  dissipative terms are neglected.
- Therefore, momentum transfer may be approximated by resistivity of fluid  $\eta$  as  $\mathbf{R}_e = \mathbf{R}_i \sim en_e \eta \mathbf{j}$  and thus heat transfer is reduced to the form  $Q_e + Q_i = -(\mathbf{u}_e - \mathbf{u}_i) \cdot \mathbf{R}_e \sim \eta |\mathbf{j}|^2$ .

By substitution of introduced quantities (2.32) under mentioned approximations and by addition of Maxwell equations in such conditions a set of resistive MHD equations is obtained

$$\frac{\partial \rho}{\partial t} + \nabla \cdot (\rho \mathbf{v}) = 0 \quad (\text{continuity}), \quad (2.33)$$

$$\rho \left( \frac{\partial \mathbf{v}}{\partial t} + \mathbf{v} \cdot \nabla \mathbf{v} \right) + \nabla p - \mathbf{j} \times \mathbf{B} = \mathbf{0} \quad (\text{momentum}), \quad (2.34)$$

$$\frac{\partial p}{\partial t} + \mathbf{v} \cdot \nabla p + \gamma p \nabla \cdot \mathbf{v} = (\gamma - 1) \eta |\mathbf{j}|^2 \quad (\text{internal energy}), \quad (2.35)$$

$$\frac{\partial \mathbf{B}}{\partial t} + \nabla \times \mathbf{E} = \mathbf{0} \quad (\text{Faraday}), \quad (2.36)$$

supplemented by

$$\mathbf{j} \equiv \mu_0^{-1} \nabla \times \mathbf{B} \quad (\text{Ampere}), \quad (2.37)$$

$$\mathbf{E}' \equiv \mathbf{E} + \mathbf{v} \times \mathbf{B} = \eta \mathbf{j} \quad (\text{Ohm}), \quad (2.38)$$

$$\nabla \cdot \mathbf{B} = 0 \quad (\text{initial condition for (2.36)}). \quad (2.39)$$

Although resistive MHD set of equations is normally used in plasma description, its simpler form of ideal MHD equations will be sufficient for further derivation. It is obtained by approximation of plasma as ideal conductor, i.e.  $\eta \rightarrow 0$ . Hence, RHS of generalized Ohm's law for conductor in motion (2.38) vanishes as well as RHS for internal energy equation (2.35). The simplest set of MHD equations then takes form

$$\begin{aligned} \frac{\partial \rho}{\partial t} + \nabla \cdot (\rho \mathbf{v}) &= 0, \\ \rho \left( \frac{\partial \mathbf{v}}{\partial t} + \mathbf{v} \cdot \nabla \mathbf{v} \right) + \nabla p - \mathbf{j} \times \mathbf{B} &= \mathbf{0}, \\ \frac{\partial p}{\partial t} + \mathbf{v} \cdot \nabla p + \gamma p \nabla \cdot \mathbf{v} &= 0, \\ \frac{\partial \mathbf{B}}{\partial t} - \nabla \times (\mathbf{v} \times \mathbf{B}) &= \mathbf{0}, \end{aligned} \quad (2.40)$$

and are supplemented by Ampère's law and condition of no magnetic monopoles

$$\begin{aligned} \mathbf{j} &\equiv \mu_0^{-1} \nabla \times \mathbf{B}, \\ \nabla \cdot \mathbf{B} &= 0. \end{aligned} \quad (2.41)$$

Generalization of hydrodynamic equations into ideal MHD equations and detailed approximation conditions may be found in [10, Goedbloed,p.67-71].

## 2.4 Static equilibrium

The goal for magnetic confined fusion is an achievement of the equilibrium, i.e. state, where magnetic pressure compensates the inner plasma pressure. By application of resistive time scale ordering [15, p.150] in order to study evolution of state described by resistive MHD equations when only slow processes are considered, i.e. velocity, time derivatives, resistive terms and source terms are of the same low order, all terms in every equation is of the same order and therefore none dominates. The only exception is the momentum equation in which the inertial term is dominated by other terms and the resulting equation

$$\nabla p = \mathbf{j} \times \mathbf{B}, \quad (2.42)$$

discuss equilibrium at the short time scale, yet allows evolution at the discussed resistive time scale. This fact is of great importance for time-evolutive numerical simulations discussed in the next chapter. Equation (2.42) sets the basis of equilibrium studies in tokamak physics. As magnetic field has a helical structure and from 2.42 current density  $\mathbf{j}$  and magnetic field  $\mathbf{B}$  are perpendicular to pressure gradient,

$$\begin{aligned} \mathbf{j} \cdot \nabla p &= 0, \\ \mathbf{B} \cdot \nabla p &= 0, \end{aligned} \quad (2.43)$$

creation of a set of nested magnetic surfaces<sup>4</sup> is mandatory for static equilibrium. Magnetic surfaces may be unambiguously characterized by pressure toroidal  $\Phi$  or poloidal  $\Psi$  magnetic fluxes. Generally used convention for many reasons<sup>5</sup> is to describe magnetic surfaces by  $\Psi$ .

Character  $\Psi$  denote function constant at magnetic surfaces and may be used for their unique description. Such function has to satisfy relation

$$\mathbf{B} \cdot \nabla \Psi = 0. \quad (2.44)$$

Magnetic field is described by rotation of vector potential  $\mathbf{A}$

$$\begin{aligned} B_R &= \frac{1}{R} \frac{\partial A_Z}{\partial \phi} - \frac{\partial A_\phi}{\partial Z}, \\ B_\phi &= \frac{\partial A_R}{\partial Z} - \frac{\partial A_Z}{\partial R}, \\ B_Z &= \frac{1}{R} \frac{\partial (RA_\phi)}{\partial R} - \frac{1}{R} \frac{\partial A_R}{\partial \phi}. \end{aligned} \quad (2.45)$$

By using vector potential  $A$  from (2.45), equation 2.44 in axis-symmetry ( $\partial/\partial\phi \rightarrow 0$ ) is easily satisfied by choice

---

<sup>4</sup>Imaginary surface including magnetic field lines

<sup>5</sup>One of them is that  $\Psi$  stands for the Hamiltonian of the system in Euler-Boozer coordinates.

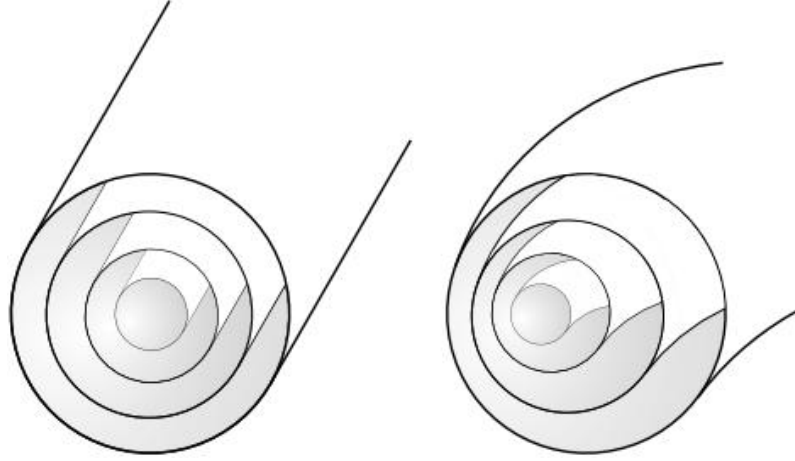


Figure 2.4: Nested surfaces for linear plasma column and for toroidal configuration with visible shift of the magnetic axis ;reprinted from [17].

$$\Psi(R, Z) = RA_\phi(R, Z) \quad (2.46)$$

This description may be used to describe magnetic field in the equation of static equilibrium (2.42). Magnetic field as function of  $\Psi$  has in cylindrical coordinates components  $B_R$  and  $B_Z$  given by equations (2.45). The remaining component might be found by calculation of integral in Ampere's circuital law

$$B_\phi = \frac{\mu_0 I(\Psi)}{2\pi R}, \quad (2.47)$$

where  $I(\Psi)$  denotes current in poloidal direction through circle of radius  $R$  limited by magnetic surface described by  $\Psi$ . Resulting magnetic field and Maxwell equations determining current density

$$\begin{aligned} B_R &= -\frac{1}{R} \frac{\partial \Psi}{\partial Z}, \\ B_\phi &= \frac{\mu_0 I(\Psi)}{2\pi R}, \\ B_Z &= \frac{1}{R} \frac{\partial \Psi}{\partial R}, \\ \mathbf{j} &= \mu_0^{-1} \nabla \times \mathbf{B}, \end{aligned} \quad (2.48)$$

is a set of equations dependant on poloidal magnetic flux  $\Psi$  describing unique magnetic

surfaces<sup>6</sup>. Continuing the derivation, by substitution of equations (2.48) into static equilibrium equation (2.42), achievement of direct plasma shape description with various initial conditions is pursued.

At first, radial and  $Z$  components of current density  $j_\phi$  and  $j_Z$  is denoted

$$\begin{aligned} j_Z &= \frac{1}{\mu_0}(\nabla \times \mathbf{B})_Z = \frac{1}{\mu_0 R} \frac{\partial}{\partial R}(R B_\phi) \equiv \frac{1}{2\pi R \mu_0} \frac{\partial}{\partial R} F(\Psi), \\ j_\phi &= \frac{1}{\mu_0}(\nabla \times \mathbf{B})_\phi = \frac{1}{\mu_0} \left( -\frac{\partial B_R}{\partial Z} + \frac{\partial B_Z}{\partial R} \right) = \\ &= -\frac{1}{2\pi \mu_0} \left( \frac{1}{R} \frac{\partial^2 \Psi}{\partial Z^2} + \frac{\partial}{\partial R} \frac{1}{R} \frac{\partial \Psi}{\partial R} \right) \equiv -\frac{1}{2\pi \mu_0 R} \Delta^* \Psi. \end{aligned} \quad (2.49)$$

Equation (2.49) is important for next explanation purposes as the theory of Green function is easily applied to it. Secondly, taking into account only radial component of equation 2.42

$$\frac{\partial p}{\partial R} = j_\phi B_Z - j_Z B_\phi, \quad (2.50)$$

and applying previously derived relations in cylindrical coordinates results in denotation

$$\begin{aligned} \frac{\partial p(\Psi)}{\partial R} + \frac{B_Z}{2\pi \mu_0 R} \Delta^* \Psi + \frac{B_\phi}{2\pi R \mu_0} \frac{\partial}{\partial R} F(\Psi) &= 0, \\ \frac{dp(\Psi)}{d\Psi} \frac{\partial \Psi}{\partial R} + \frac{B_Z}{2\pi \mu_0 R} \Delta^* \Psi + \frac{B_\phi}{2\pi R \mu_0} \frac{dF(\Psi)}{d\Psi} \frac{\partial \Psi}{\partial R} &= 0, \times \frac{2\pi \mu_0 R}{B_Z}, \\ \Delta^* \Psi + 4\pi^2 \mu_0 R^2 \frac{dp}{d\Psi} + F(\Psi) \frac{dF(\Psi)}{d\Psi} &= 0. \end{aligned}$$

By expansion of operator  $\Delta^*$ , called elliptical operator, important Grad-Shafranov equation is obtained, [15]

$$R \frac{\partial}{\partial R} \left( \frac{1}{R} \frac{\partial \psi}{\partial R} \right) + \frac{\partial^2 \psi}{\partial Z^2} = -\mu_0 R^2 \frac{\partial p}{\partial \Psi} - F(\Psi) \frac{\partial F(\Psi)}{\partial \Psi}, \quad (2.51)$$

where  $\Psi$  is the magnetic poloidal flux,  $r$  and  $z$  stand for cylindrical coordinates<sup>7</sup>.

Grad-Shafranov equation is a two-dimensional, nonlinear, elliptic, partial differential equation for variable  $\Psi$ , which is both dependent and independent variable in this equation. Assumptions in the derivation were axis-symmetry of the problem and low frequencies of events so Maxwell displacement current was neglected and Coulomb gauge for steady fields was used.

<sup>6</sup>As these surfaces enclose constant magnetic flux, terminology of flux surfaces is used as well.

<sup>7</sup> $\phi$  vanished from the equation thanks to the tokamak axis-symmetry

## The need of vertical magnetic field

The Grad-Shafranov equation (2.51) solution describes what form does the equilibrium takes under given currents in poloidal coils and profiles of current (function  $F(\Psi)$  depends on radial coordinate and current through equatorial area associated to  $\Psi$ ) and pressure. Yet if there was only poloidal and toroidal magnetic field, the plasma ring would create a dipole layout, with stronger poloidal field at HFS and weaker at the LFS. As in toroidal configuration exist forces on the plasma column, e.g. hoop force, expanding the ring towards the LFS, such layout would not be able to achieve equilibrium. Therefore, vertical field inverting the situation, i.e. weakening poloidal field at HFS and strengthening it on LFS, is implicitly hidden in Grad-Shafranov equation and is essential for plasma confinement in tokamaks.

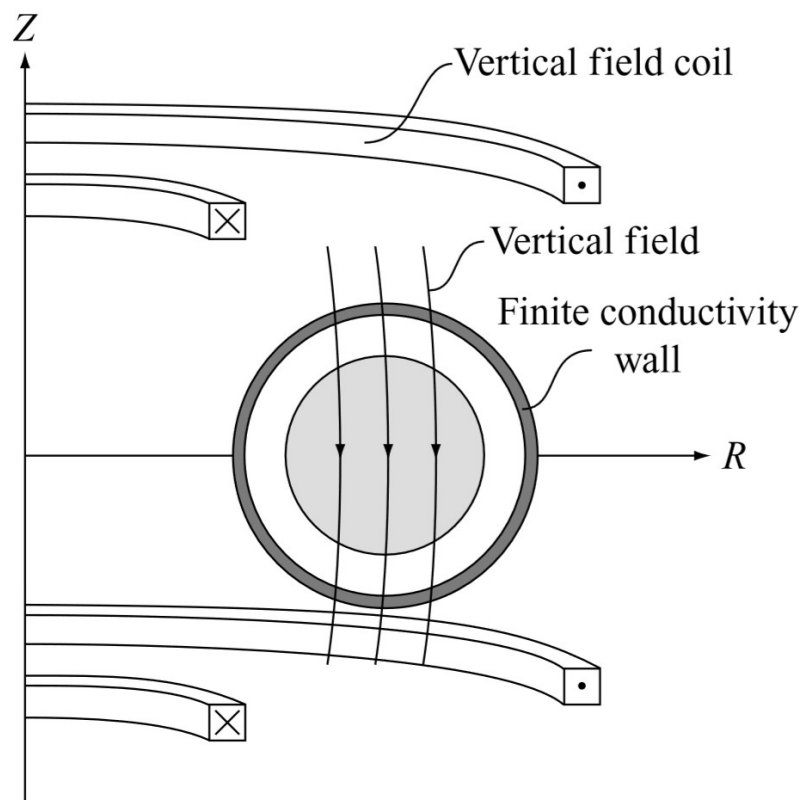


Figure 2.5: Visualisation of necessary vertical field and its source coils; reprinted from [9].

In the specific case of circular plasma is possible to find analytic solution for the vertical field  $B_V$  in the form of

$$B_V = -\frac{\mu_0 I_p}{4\pi R_0} \left( \ln \frac{8R_0}{a} - \frac{3}{2} + \beta_p + \frac{l_i}{2} \right) \sim I_p \left( \beta_p + \frac{l_i}{2} \right), \quad (2.52)$$

where  $l_i$  is the normalized internal plasma inductance and  $\beta_p$  is defined as a mean plasma pressure  $p$  divided by the poloidal component of a magnetic field  $B_p$

$$\beta_p = 2\mu_0 \frac{\langle p \rangle}{B_p^2}. \quad (2.53)$$

# Chapter 3

## Plasma simulations

“Essentially, all models are wrong, but some are useful.”

- G.E.P.Box & N.R.Draper, [4, p.424]

Any physics law describes our world by variables easily understood by a human mind, yet it still remains a model describing reality. Similarly, with a drawback of computational power, numerical simulations exploit theoretical equations to model the reality. Although it might look like as redundant work, numerical methods give insight into solution of analytically unsolvable equations. Grad-Shafranov equation derived in chapter 2.4 is a nonlinear partial differential equation and stands as such challenge, where numerical code is necessary. By carefully specifying conditions and limitations of our model the result will correspond to the reality to a certain degree of precision and may be useful, nevertheless it cannot perfectly describe the reality of our world.

However, as experiment information yield is usually superior to the one of a numerical model, consideration of a need for numerical model is only logical. Most knowledge can be obtained by observation or experiment, yet there are systems limited by dimension, e.g. sub-atomic research, or their conditions<sup>1</sup>. Furthermore, economic reasons of large experiments often lead to the development of a model in order to predict partial results and reduce its operational cost. Following section discuss modern tokamaks as such a case.

### 3.1 Scaling laws

As mentioned in chapter 1.2, Lawson criterion (1.13) respectively the triple product condition (1.15) set basic limits for fusion power-plant to operate. A way towards its fulfilment in tokamaks may be clarified by considering its elements one by one: The

---

<sup>1</sup>Nebulae conditions are hard to simulate in the gravitational field of Earth

ideal temperature for the operation with is known (chapter 1.2) and the plasma density is limited by its pressure<sup>2</sup> given by parameter  $\beta$  denoting ratio between plasma pressure and the one of magnetic field  $B$

$$\beta = \frac{p}{p_{mag}} = \frac{nk_B T}{B^2/(2\mu_0)}. \quad (3.1)$$

In fact, beta is a limited variable as well, specifically by the Troyon limit, [9, Freidberg,p.397]

$$\beta_{max} = \frac{\beta_N I}{a B_0}, \quad (3.2)$$

where  $\beta_N$  is a numerical constant usually given as 2.8 if the limit  $\beta_{max}$  is a percentage<sup>3</sup>. As the numerical nature of  $\beta_N$  suggests, the Troyon limit is a experimental restriction usually dividing values of unstable plasmas.

Hence, two possible ways of fulfilling the triple product condition are higher density limits achieved by stronger magnetic field and the energy confinement time  $\tau_E$  defined as (1.5). Both approaches have their benefits and limitations. Greater magnetic field stress the support structure of the tokamak and limit possible use of superconductors for coils<sup>4</sup>, yet achieves better densities and small dimensions of the device at the same time. The other way is improvement of the confinement time.

The energy confinement time quantity may be theoretically calculated by certain models, e.g. by particle random walk. Prediction of such complex variable is a challenge in nowadays tokamak physics and there are many aspects to consider in the calculations. As an example, plasma turbulences are one of the major ones and various simulations try to understand and predict them. Gyrokinetic simulations and simplified first-principle transport models are the present state-of-the-art in describing the turbulent transport in tokamak plasmas. However, the actual results are not capable of fully explaining experimental results. Complementary to theoretical efforts, heuristic scaling laws based on fitting of experimental data, provide a practical insight into tokamak confinement properties. For example, the ITER Physics Basis (IPB) scaling for ELMy H-modes is [24]

$$\tau_E^{ELMy} = 0.05621 I_p^{0.93} B^{0.15} P_H^{-0.69} n^{0.41} M^{0.19} R^{1.97} \epsilon^{0.58} \kappa_a^{0.78}, \quad (3.3)$$

where  $I_p$  stands for plasma current,  $B$  for magnetic field,  $P_H$  represents the heating power,  $n$  plasma density,  $M$  average ion mass,  $R$  large radius of the tokamak and  $\epsilon$  and  $\kappa$  plasma elongation and triangularity respectively. The highest power suggests the way for fulfilling the triple product condition by increasing the tokamak radius.

---

<sup>2</sup>In simple approximation given by ideal gas law

<sup>3</sup> $\beta_N = 0.028$  when fraction description is used

<sup>4</sup>Superconductor is characterized by its limit magnetic field function  $B(T)$  limiting its superconducting properties.

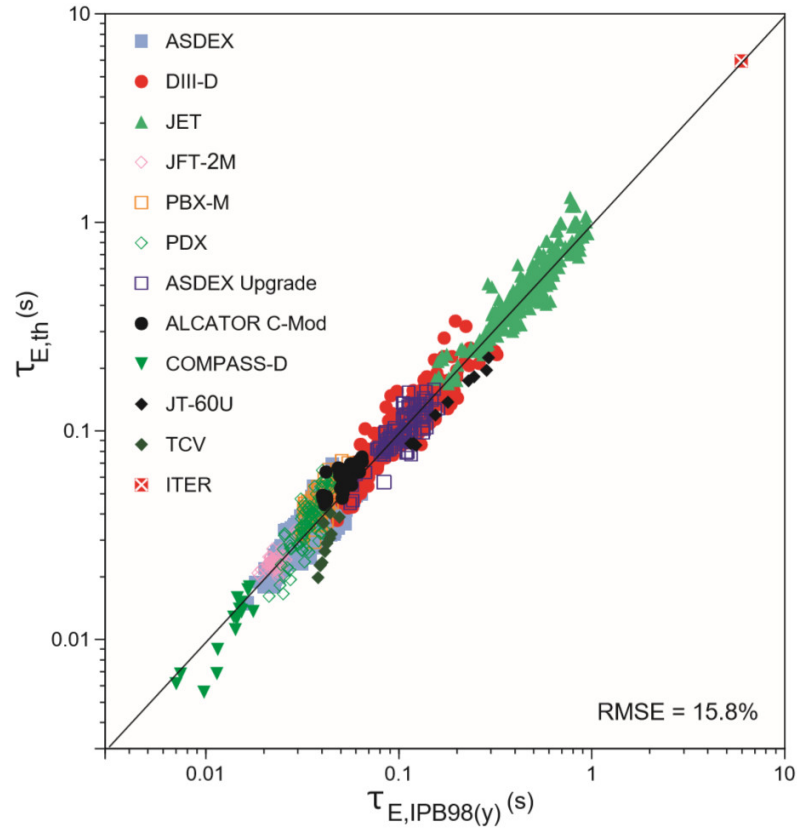


Figure 3.1: Fitting of the energy confinement time experimental results; reprinted from [24, ITER Physics Basis vol.2, p.2205].

Even by inventing any improvements bringing minor variation to the fit dependency, the main characteristic remains the same: the triple product function rises with the radius  $R$  of a tokamak. Due to this fact, scaling of tokamaks is necessary and leads to projects like JET, ITER and DEMO. By scaling the projects, their maintenance costs rises as well and therefore the simulations of discharges are necessary in order to partially predict the results and lower the research reactor maintenance cost. Moreover, even during the device design itself is numerical modelling a key step for technical limits prediction.

## 3.2 Integrated modelling

As a very complex system, plasma is difficult for simulation. While considering the computational power of humanity nowadays, the simulation that would cover the whole

state space (time, position and velocity) cannot describe large number of particles as standalone objects. Therefore, various codes based at different approximations are necessary to study plasma. Moreover, modelled phenomena differ at scale of both, spatial and temporal, dimensions. An example are MHD simulations describing macroscopic phenomena, whereas gyrokinetic particles study transport and are based on individual movement. Although various simulations can yield important, correct results, they operate only at a domain, i.e. time and space scale, limited by previous approximations. In order to verify its functionality, it has to be benchmarked to an already verified code on the overlapping domain, e.g. code describing movement of single particles should yield the same results as a code describing collective movement of plasma, when the amount of particles that both codes can handle is tested. Benchmarking of codes is a crucial step for plasma simulation.

As the need for numerical simulations of plasma arise for large fusion experiments like JET, ITER and DEMO, a lot of codes describing one particular aspect of the discharge were written. Hence, The European Work Package Code Development (WPCD), formerly the Integrated Tokamak Modelling (ITM) EFDA taskforce, [8], or its ITER analogy—the Integrated Modelling and Analysis Suite (IMAS, [13])—were founded with the aim of simulations coordination. Their main goal is to provide simulation framework providing standardized suite of validated numerical codes for the simulation and prediction of a complete plasma discharge. As such codes vary in described dimensions, e.g. MHD codes describe evolution of plasma column whereas particle modelling is used for plasma-material interaction, a need for standardized output and input emerged. Therefore, WPCD and IMAS are based on a generic data structure and its elements are labelled as Consistent Physical Objects (CPO), [13]. By normalizing the inputs and outputs of individual codes, a seamless coupling of individual components was possible and work-flow of the global simulation was discussed. In order to allow easy benchmarking of individual numerical codes contributing to the global suite of codes, a modular structure for different physics topics was adopted. Hence, easy substitution of individual numerical codes for each physics part was possible and therefore its mutual benchmarking was straightforward. Moreover, comparison with data from experiment needs only its translation into CPO structure. Not only discharge data were unified by WPCD and IMAS yet standardized Machine Descriptions (MD) were introduced allowing easy device data acquisition and therefore testing of codes under development at various devices.

The most complex WPCD project, which couples numerous WPCD modules, is the European Transport Solver (ETS), [6]. It is designed to simulate the time evolution of a tokamak discharge. One of the core components of ETS are an equilibrium solver coupled with a transport equations solver. Basically, the (static) equilibrium solver provides the flux surface geometry for time-dependent transport equations, whereas transport equation provides time evolution of the system for the equilibrium solver. Extending this program core, various modules might incorporate more phenomena to the simulation, e.g. Neutral Beam Injection (NBI), Ion Cyclotron Resonant Heating (ICRH), plasma-wall interactions.

All modules are one by one complex simulations, yet this thesis discuss one of the core ones - equilibrium. The availability of equilibrium codes was recently extended by Free Boundary Equilibrium Solver, FREEBIE, [3].

### 3.3 FREEBIE

The Grad-Shafranov equation may be solved as fixed boundary problem, i.e. with a given plasma shape and boundary conditions. These are usually the Neumann boundary condition on the total current [25].

On the other hand, a free boundary problem is characterized by not imposing directly the plasma boundary. This implies that another additional information of the system is necessary. This need is primarily satisfied by information of currents in poloidal tokamak systems (active and passive), dominantly poloidal field coils.

The FREEBIE code implements this approach to simulate plasma in a more complex way. Its code development started at CEA Cadarache and was stand-alone benchmarked for TCV and ITER. After such successful milestone, CEA went on with the development of the code by adding additional modes of FREEBIE, i.e. the inverse and the unique Poynting modes.

The inverse mode does not utilize the additional condition of currents in poloidal systems of tokamak, yet replaces it with constrains on the plasma shape. By replacing the conditions, the program does not obtain currents time evolution from circuit equations. Instead, FREEBIE iterates for the current distribution in the inverse mode (see fig.3.2) and circuit equations are replaced by an optimizer, which minimizes certain quantities in the solution, e.g. error in the boundary flux.

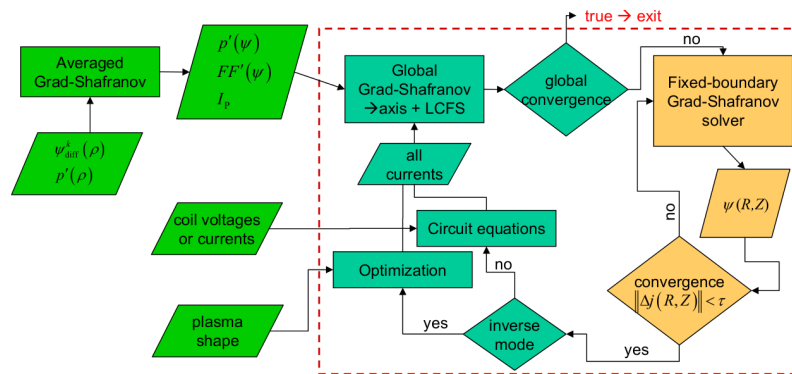


Figure 3.2: Scheme of the FREEBIE code, [25]

In FREEBIE, the solution of the free-boundary problem extends the fixed-boundary

problem and the code is implemented to use internally de facto any fixed-boundary solver. This solver has a condition on its boundary in every iteration of FREEBIE. FREEBIE itself iterates in all operation modes until the global convergence criterion is satisfied.

By satisfaction of the global convergence, the FREEBIE module grants an output of magnetic equilibrium. When coupled with a transport code, FREEBIE is called in every time step. Therefore, the time evolution description of plasma is possible as a sequence of MHD equilibria (the problem is considered as quasi-static) and transport equations solutions [14]. In this meaning, the microscopic MHD equilibrium satisfied in stationary plasma results in macroscopic evolution of plasma shape.

In detail, the FREEBIE code solves the non-linear Grad-Shafranov PDE by usage of the Green function [2]. By applying the Green function theory on the Grad-Shafranov equation (2.49), the solution of PDE may be obtained as convolution of previously calculated Green function with the source term, i.e. RHS of the equation when differential operator stands alone at LHS.

$$\psi(R, Z) = \int_P G(R, Z; R', Z') j_\varphi dR' dZ' + \sum_{i=1}^{N_c} G(R_i^c, Z_i^c; R', Z') I_\varphi, \quad (3.4)$$

where  $\psi$  is the poloidal magnetic flux variable used in initial equation (2.49),  $R, Z$  are coordinates describing the poloidal cross-section of the tokamak,  $j_\varphi$  stands for the toroidal current density in plasma,  $N_c$  is the number of poloidal components (active and passive),  $G$  stands for the Green function and  $I_\varphi$  stands for the currents in poloidal components. The integral limit is the plasma boundary, i.e. we integrate over the whole plasma column. The  $j_\varphi$  variable is not precisely specified as in the program itself FREEBIE discretizes the integral into plasma segments. This is done by a triangular grid with high resolution (usage example is on fig.3.3) and equation (3.4) then takes form of

$$\psi(R, Z) = \sum_{i=1}^N G(R, Z; R_i^p, Z_i^p) j_{\varphi i} + \sum_{i=1}^{N_c} G(R, Z; R_i^c, Z_i^c) I_{\varphi i}, \quad (3.5)$$

where  $N$  stands for number of elements plasma is divided into.

The grid is calculated in the initial phase of the program by exploitation of the graph theory and is therefore optimized for the problem. On this grid, the Green function may be pre-calculated and the solution is therefore much faster.

Yet, as a new tool in the WCPD effort, the FREEBIE code is still in development. This thesis goals are meant to support this development and contribute to FREEBIE by a yield of adequate results.

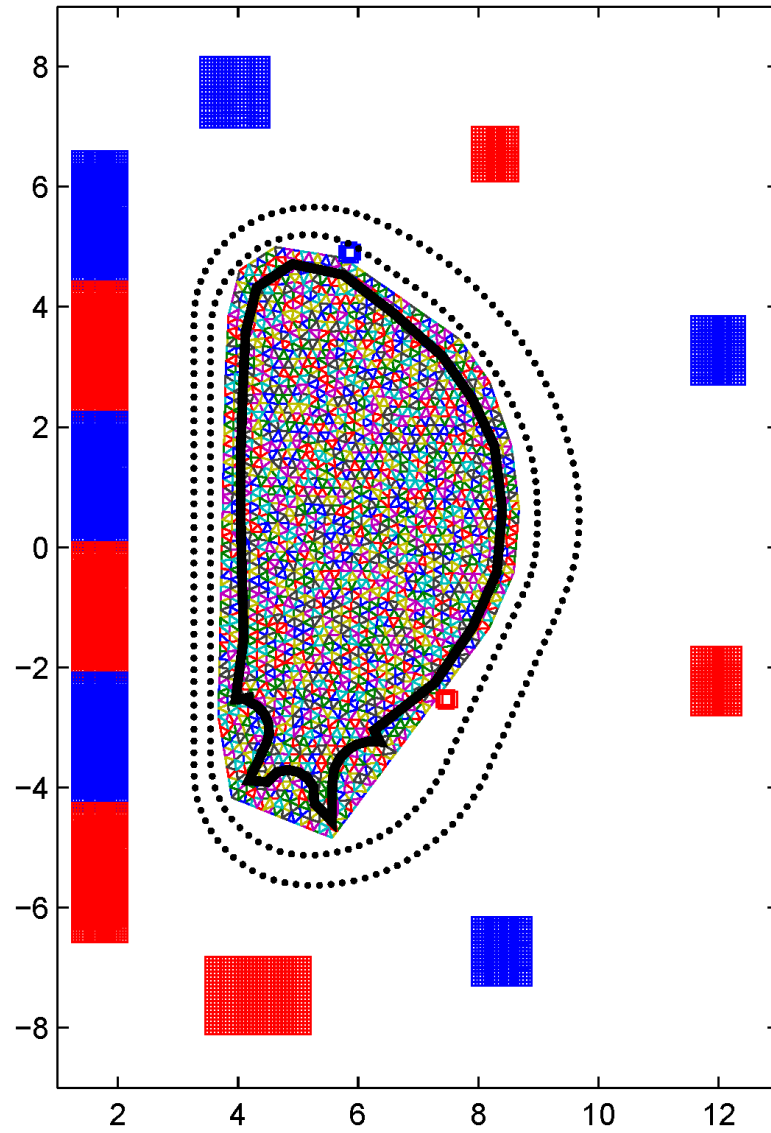


Figure 3.3: An example of triangular grid usage by FREEBIE code; reprinted from [16].

# Chapter 4

## Results

The results of this thesis discuss few not strictly bonded topics: A new solver of general electrical circuits for FREEBIE, which is necessary for simulating complex PF circuits. Using WPCD CPO specifications, I have created a machine description of the COMPASS Upgrade (COMPASS-U) tokamak and made static equilibrium simulations for various plasma shapes and kinetic profiles. Starting with these static equilibria, I have simulated vertical displacement events (VDE's) for the COMPASS-U tokamak, which set requirements on the vertical position feedback system. Moreover, I have created a post-processing module `equi2d.py` that can facilitate further usage of equilibrium codes outputs.

### 4.1 General electrical circuits solver

So far, the FREEBIE program was able to describe the poloidal system of coils in tokamak as separated series electrical circuits of an applied voltage and coils. However, in general may circuits be more complex, e.g. poloidal systems power supply circuit at the COMPASS tokamak visualized in the fig.4.1.

So far, circuit equations describing the PS within the FREEBIE program used the matrix description in order to apply specific solvers of such systems, e.g. eigenvalues decomposition and reducing the solution by eigenvalues of less importance. This description

$$\mathbf{V} + \overleftrightarrow{R} \cdot \mathbf{I} + \overleftrightarrow{L} \frac{d\mathbf{I}}{dt} = \mathbf{0}, \quad (4.1)$$

where  $\mathbf{V}$ ,  $\mathbf{R}$  and  $\mathbf{I}$  stand for the voltage, resistance and current vectors (resistance is a matrix with only diagonal elements, so the final dimension of multiplication yields a vector), describe circuits as by Kirchhoff circuital law. The voltage is not only the applied voltage, but its addition with the one induced in circuits by plasma<sup>1</sup>. They are all of

---

<sup>1</sup>Plasma can be understood as an additional coil with inhomogeneous material and therefore resistance

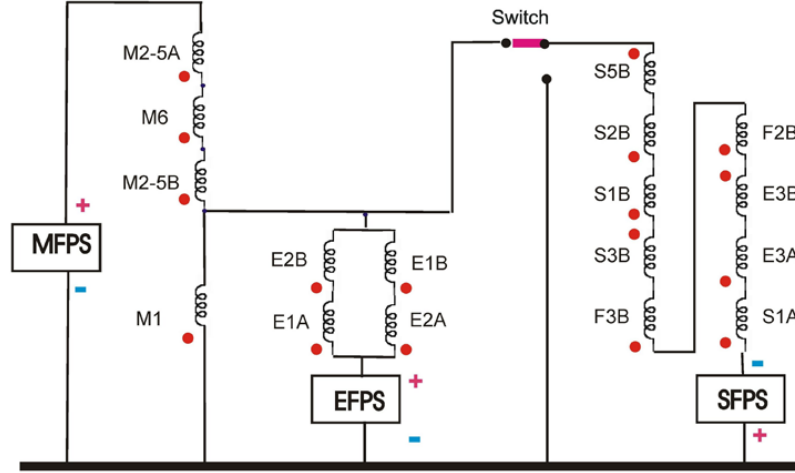


Figure 4.1: Scheme of the real COMPASS circuit for the poloidal systems, [1].

dimension  $n$ , the number of components to be described. The matrix  $L$  is the inductance matrix describing the coils and passive structures self/mutual inductance. This solver has no way how to add the information about the complex circuits, e.g. the parallel components. Moreover, series circuits are pre-calculated into simple forms, i.e. series coils are treated as one with summed resistance.

Such solver limits the application of the program and therefore its replacement was at hand. In order to describe such circuit, an additional information has to be brought to the system. This information should describe the nodes and their mutual relations. The solution may be found by studying the Kirchhoff voltage law:

**KVL:** The voltage drop around any loop is zero.

The voltage drop is the difference of potentials, which are the desired solution of the problem. Potentials may be used to describe every node and their mutual relations (potential difference due to element between nodes). The system of circuit equations (4.1) may be therefore rewritten in a way of potential description, suggested by the CEDRES team in [12].

$$\overleftrightarrow{A}\mathbf{U} = \overleftrightarrow{B}\mathbf{V} + \overleftrightarrow{R}\mathbf{I} + \overleftrightarrow{L}\frac{d\mathbf{I}}{dt}, \quad (4.2)$$

where  $\mathbf{U}$  is a vector of potentials at each node of the circuit,  $\mathbf{I}$  is the vector of currents in circuit components,  $\mathbf{V}$  stands for power supplies voltages in the set of equations, and  $\overleftrightarrow{A}$ , and inductance. This issue may be solved by dividing plasma into discrete elements.

$\overleftrightarrow{B}$ ,  $\overleftrightarrow{R}$  and  $\overleftrightarrow{L}$  are potential, voltage, resistance and inductance matrices respectively. The most important term in this algorithm is the potential (connection) matrix  $\overleftrightarrow{A}$ , describing general circuit connection by values of  $\{1, 0, -1\}$ . Exemplary matrix describing two separated circuits of one power supply and one coils each follows

$$\overleftrightarrow{A} = \begin{pmatrix} \left\{ \begin{array}{cccc} 1 & -1 & 0 & 0 \\ 0 & 0 & 1 & -1 \end{array} \right. \\ \left\{ \begin{array}{cccc} 1 & -1 & 0 & 0 \\ 0 & 0 & 1 & -1 \end{array} \right. \\ \left\{ \begin{array}{cccc} 0 & 0 & 0 & 0 \\ 0 & 0 & 0 & 0 \\ 0 & 0 & 0 & 0 \\ 0 & 0 & 0 & 0 \end{array} \right. \\ \left\{ \begin{array}{cccc} 0 & 1 & 0 & 0 \\ 0 & 0 & 0 & 1 \end{array} \right. \end{pmatrix} \quad (4.3)$$

In matrix  $\overleftrightarrow{A}$ , the first part describes the potentials drop at each component, e.g. for a coil between nodes  $i$  and  $k$  specified by their potentials

$$U_i - U_k = \overleftrightarrow{R}_i \mathbf{I} + \overleftrightarrow{L}_l \frac{d\mathbf{I}}{dt}, i, k \in \hat{n}, i \neq k, l \in \hat{m}, \quad (4.4)$$

where  $\hat{n}$  stands for a set from one to the number of nodes  $n$  and  $\hat{m}$  stands for a set from one to the  $m$ , which is the other dimension of matrix A, i.e. addition of number of components, number of coils and number of circuits as described in following text. The second part of matrix  $\overleftrightarrow{A}$  is empty due to the whole equation set (4.2) dimension. These equations describe the Kirchhoff's current law in each coil by matrix  $\overleftrightarrow{R}$ . The last equations are definitions of ground potentials for each circuit.

The notable change between (4.1) and (4.2) is that resistance is no longer vector (pure diagonal matrix), but matrix in a normal way. Reason of this fact is easily seen when the dimension analysis of this equation is made. The desired  $\mathbf{I}$  is vector of currents in every component, e.g. coils and passive structures, of dimension  $n_{comp}$ . In our new system of equations (4.2), there are  $n_{nodes}$  new variables  $\mathbf{U}$ . For each of those variables, another equation is needed in order to keep the system regular. Easily obtained equations of same count are Kirchhoff nodal (current) equations. This is the reason for the matrix shape of resistance variable as this additional laws are described in it. Yet, the problem of potentials is the necessity of setting the zero potential in each described circuit. This yields another  $n_{circuit}$  equations. The system is therefore dependent and may be narrowed by  $n_{circuit}$  equations, usually taken from the Kirchhoff current law ones.

As the coefficient matrices are by default not square, the derivation of an equation for the current vector is not straightforward. First step is to express vector  $\mathbf{U}$  and plug it back in the system. Even though connection matrix  $\mathbf{A}$  is not square, the multiplication with its transpose version is. Such a square matrix may be finally inverted. In this way the potential vector is expressed and by plugging it into the original system of equations (4.2) we can derive matrix description without the potential vector, yet still obtaining the connection matrix information

$$\mathbf{0} = \overleftrightarrow{E} \mathbf{V} + \overleftrightarrow{F} \mathbf{I} + \overleftrightarrow{G} \frac{d\mathbf{I}}{dt}, \quad (4.5)$$

$$\begin{aligned} \overleftrightarrow{E} &= \overleftrightarrow{A} (\overleftrightarrow{A}^T \overleftrightarrow{A})^{-1} \overleftrightarrow{A}^T \overleftrightarrow{B} - \overleftrightarrow{B}, \\ \overleftrightarrow{F} &= \overleftrightarrow{A} (\overleftrightarrow{A}^T \overleftrightarrow{A})^{-1} \overleftrightarrow{A}^T \overleftrightarrow{R} - \overleftrightarrow{R}, \\ \overleftrightarrow{G} &= \overleftrightarrow{A} (\overleftrightarrow{A}^T \overleftrightarrow{A})^{-1} \overleftrightarrow{A}^T \overleftrightarrow{L} - \overleftrightarrow{L}. \end{aligned} \quad (4.6)$$

By following similar steps, the vector  $\mathbf{I}$  in the following form may be derived

$$\mathbf{I} = \overleftrightarrow{S} \mathbf{V} + \overleftrightarrow{T} \frac{d\mathbf{I}}{dt}, \quad (4.7)$$

$$\begin{aligned} \overleftrightarrow{S} &= -(\overleftrightarrow{F}^T \overleftrightarrow{F})^{-1} \overleftrightarrow{F}^T \overleftrightarrow{E}, \\ \overleftrightarrow{T} &= -(\overleftrightarrow{F}^T \overleftrightarrow{F})^{-1} \overleftrightarrow{F}^T \overleftrightarrow{G}. \end{aligned} \quad (4.8)$$

where  $\overleftrightarrow{S}$  and  $\overleftrightarrow{T}$  are altered voltage and inductance matrices, which include information about resistances of coils and their connection, i.e. matrices  $\overleftrightarrow{A}$  and  $\overleftrightarrow{R}$  in original formula.

Results of previous testing of the algorithm on simple circuits with easy analytical solutions may be found in [21]. They verified the solver as the numerical values followed the analytical solutions precisely.

The solver itself experienced internal errors when more serial components were considered. This was caused by a combination of differential equations describing element voltage drop and Kirchhoff's node law algebraic equations resulting in singular inductance matrix. Therefore, I have implemented procedure eliminating algebraic equations by substitution of variables and solving these equations independently after each time step of calculation. That means the solver search for independent currents only and calculate the other from necessary Kirchhoff laws.

The described circuit equation solver is not yet fully integrated into FREEBIE because of technical complications. In particular, the assumption on purely serial coil connections is present in multiple FREEBIE functions and variables.

Such solution allowed processing of serial circuits and finally the complex circuits of poloidal field coils power supply at the COMPASS tokamak, where the most complicated one is visualized in 4.1. Although import of the data from FREEBIE description of the

COMPASS tokamak would lead to relevant results, inductance matrix which is necessary as input in the general solver are calculated internally in FREEBIE and its dimension mismatch matrix of the solver. As stated above, the FREEBIE solver considered so far only series circuits, with no dissipation of the current and therefore the calculations were made for the number of currents equal to the number of circuits. Moreover, inductances for individual series coils were merged and calculated as one and therefore reducing the dimension of matrices and thus the computational time.

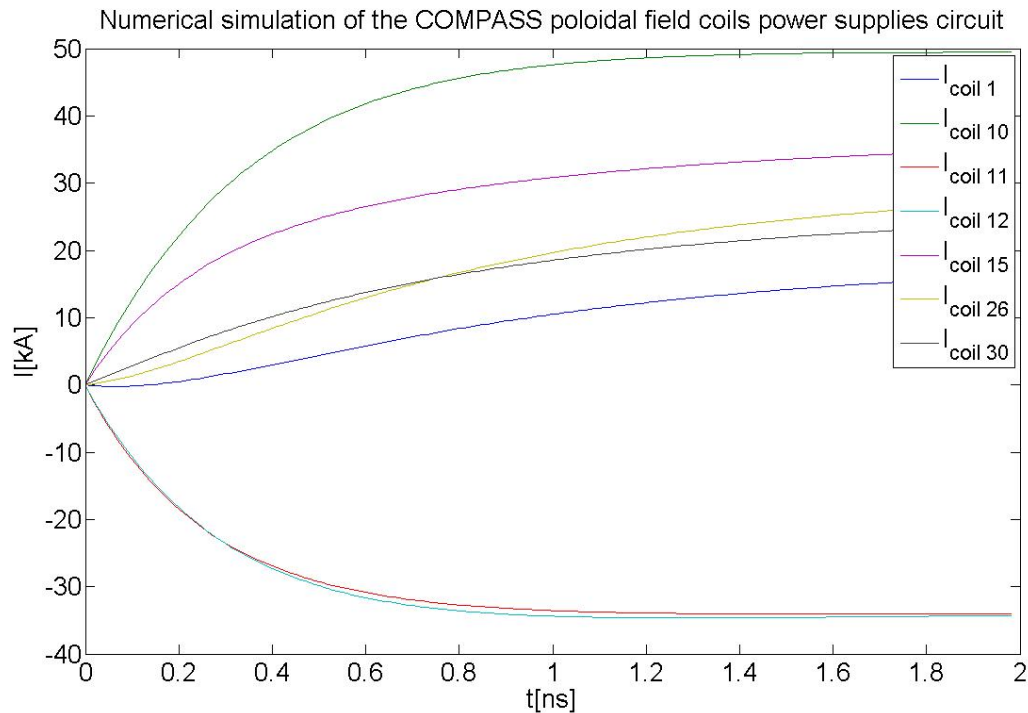


Figure 4.2: Result of simulation run by general electrical circuit solver with random scaled inductances visualizing seven different current values for seven unique branches in the poloidal field coils power supply system.

Presently, the solver can deal with COMPASS relevant data. The result of the general circuits solver for COMPASS, although with artificial inductances, is shown in figure 4.2. Most important is the fact that the solver calculation for all 33 coils results in 7 distinguishable currents according to the total of 7 circuit branches<sup>2</sup>.

---

<sup>2</sup>5 for the circuit visualized in 4.1 plus separate vertical and horizontal field circuits.

## 4.2 COMPASS-U

COMPASS is a moderate size tokamak which features ITER relevant design and extended experimental variability. In order to extend its lifetime and keep up with cutting-edge fusion research, an upgrade, COMPASS-U, is presently considered. The main COMPASS-U features are a high magnetic field (up to 5 T), larger yet still compact size and an extended heating power. In pursuance of minimal risks for the operation of COMPASS-U, significant simulation effort is necessary during its design. Among the most important simulations stands free-boundary equilibrium with results of plasma configuration consistent with hardware limits and vice versa.

### 4.2.1 Static equilibria

Following the ITM-TF effort of data structures unification, I have created a CPO structure for the COMPASS-U as the input for the FREEBIE program. Initial data for the CPO were obtained from previous FIESTA [7] (which is a different free-boundary equilibrium code) simulations for COMPASS-U.

After initialization of a new virtual device in the FREEBIE program, characteristic plasma shapes were tested. Specifically, a circular plasma limited at HFS of the tokamak, elongated plasma restricted in the same way and a large, D-shaped plasma with an X-point. All configurations were successfully simulated by the FREEBIE inverse calculation procedure for the static equilibria solution. The resulting values of the current in poloidal field coils are shown in the table 4.1. Significant differences in the required currents are obvious. Poloidal cuts of the flux surfaces together with the tokamak structure and PF coils are visualized in figures 4.3, 4.4 and 4.5. In the table are highest values formatted as bold text, providing the current requirement for COMPASS-U poloidal field coils necessary to achieve given plasma shapes. As expected, the strongly shaped plasma requires the largest local currents. Resulting values need to be considered as minimal requirement for the poloidal field coils design, yet safety factors and technical limits are necessary for the real design.

|                  | Circular       | Elongated      | Shaped         |
|------------------|----------------|----------------|----------------|
| $I_{coil1}[kA]$  | -17.483        | -17.690        | <b>22.853</b>  |
| $I_{coil2}[kA]$  | -6.438         | -17.022        | <b>-38.872</b> |
| $I_{coil3}[kA]$  | -6.222         | <b>-17.096</b> | -1.222         |
| $I_{coil4}[kA]$  | -16.989        | -17.174        | <b>-24.342</b> |
| $I_{coil5}[kA]$  | -8.512         | -4.595         | <b>12.047</b>  |
| $I_{coil6}[kA]$  | -8.380         | -4.434         | <b>10.720</b>  |
| $I_{coil7}[kA]$  | <b>-11.826</b> | 1.108          | 0.800          |
| $I_{coil8}[kA]$  | -11.933        | 0.978          | <b>38.006</b>  |
| $I_{coil9}[kA]$  | -6.088         | <b>11.213</b>  | -4.463         |
| $I_{coil10}[kA]$ | -6.656         | 10.778         | <b>-40.259</b> |
| $I_{coil11}[kA]$ | -11.646        | <b>-28.008</b> | -16.949        |
| $I_{coil12}[kA]$ | -10.906        | <b>-27.296</b> | -6.464         |
| $I_{coil13}[kA]$ | <b>-8.593</b>  | 5.751          | -6.236         |
| $I_{coil14}[kA]$ | -8.883         | 5.416          | <b>21.441</b>  |

Table 4.1: Poloidal field coils currents calculated by inverse mode of FREEBIE for circular, elongated and shaped plasma. The highest value for individual coils are bold, providing technical requirement for the COMPASS-U.

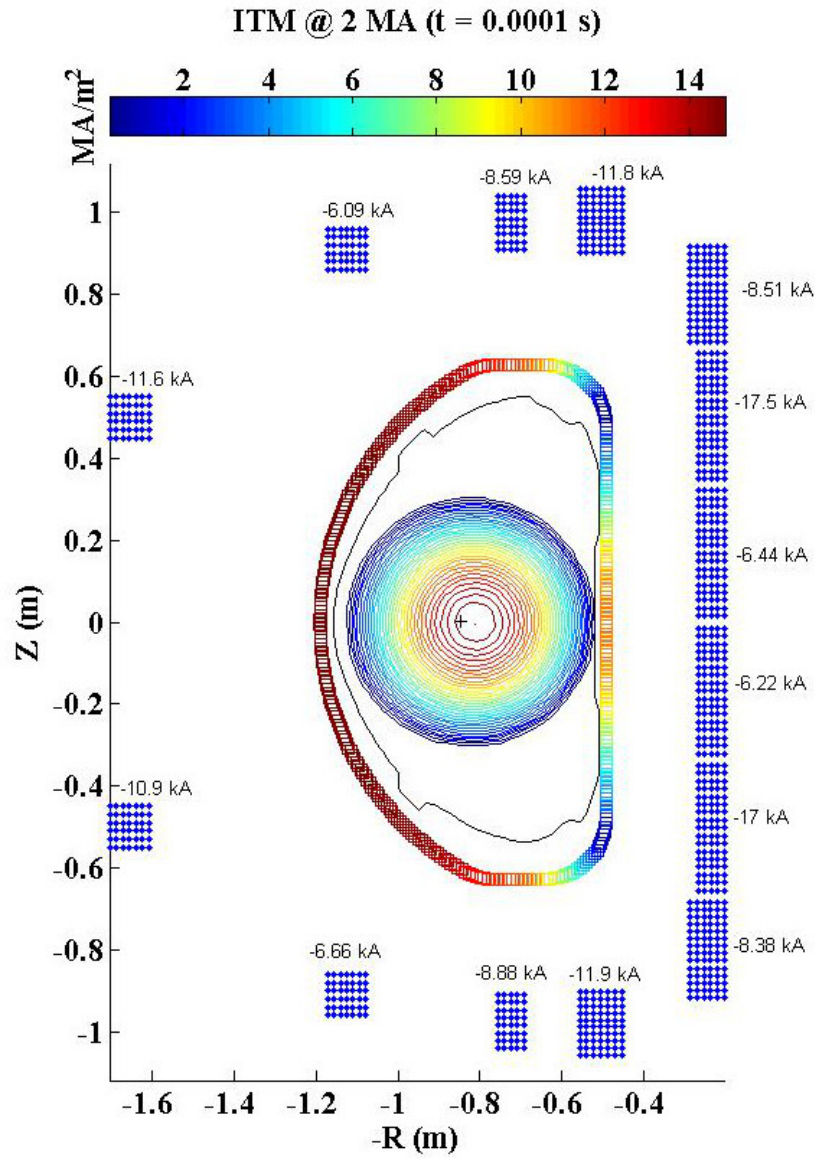


Figure 4.3: Plasma current density  $\mathbf{j}_\phi$  (contours), poloidal field coils and the vessel structures of COMPASS-U calculated by FREEBIE inverse mode for circular plasma shape.

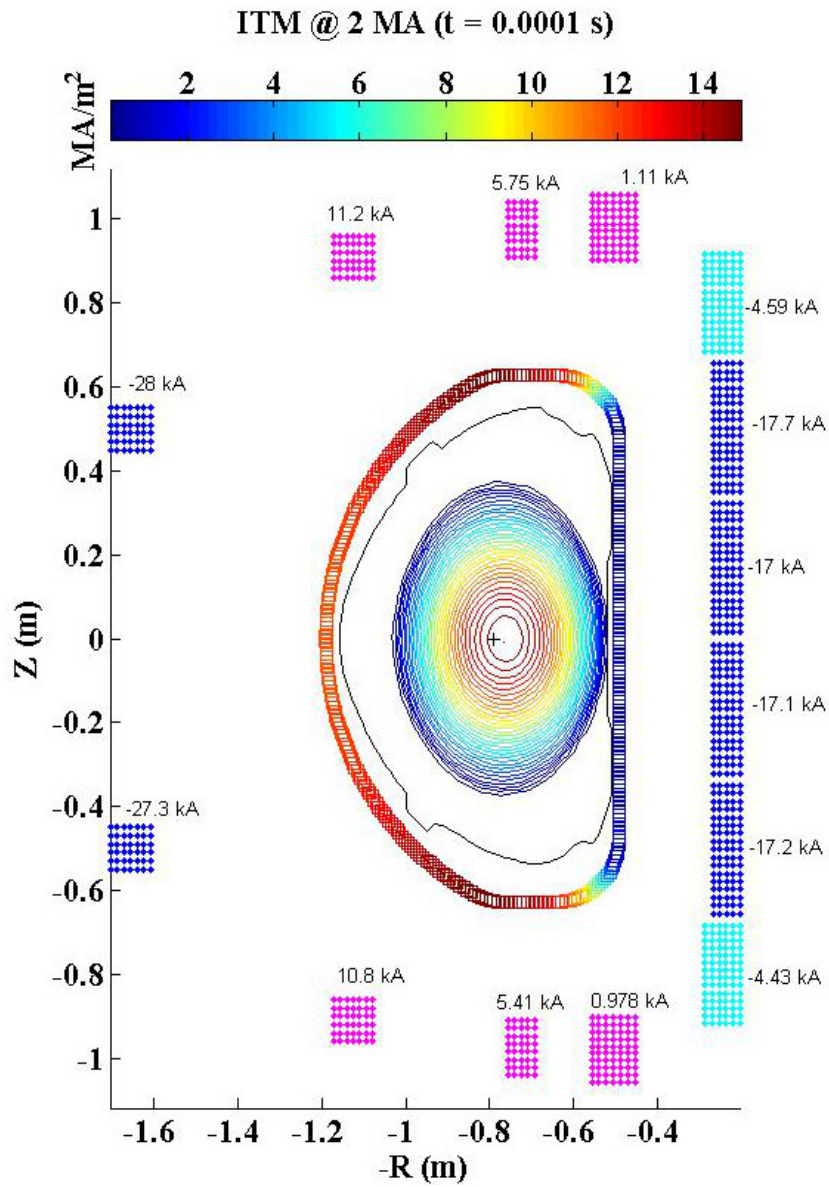


Figure 4.4: Plasma current density  $j_\phi$  (contours), poloidal field coils and the vessel structures of COMPASS-U calculated by FREEBIE inverse mode for elongated plasma shape.

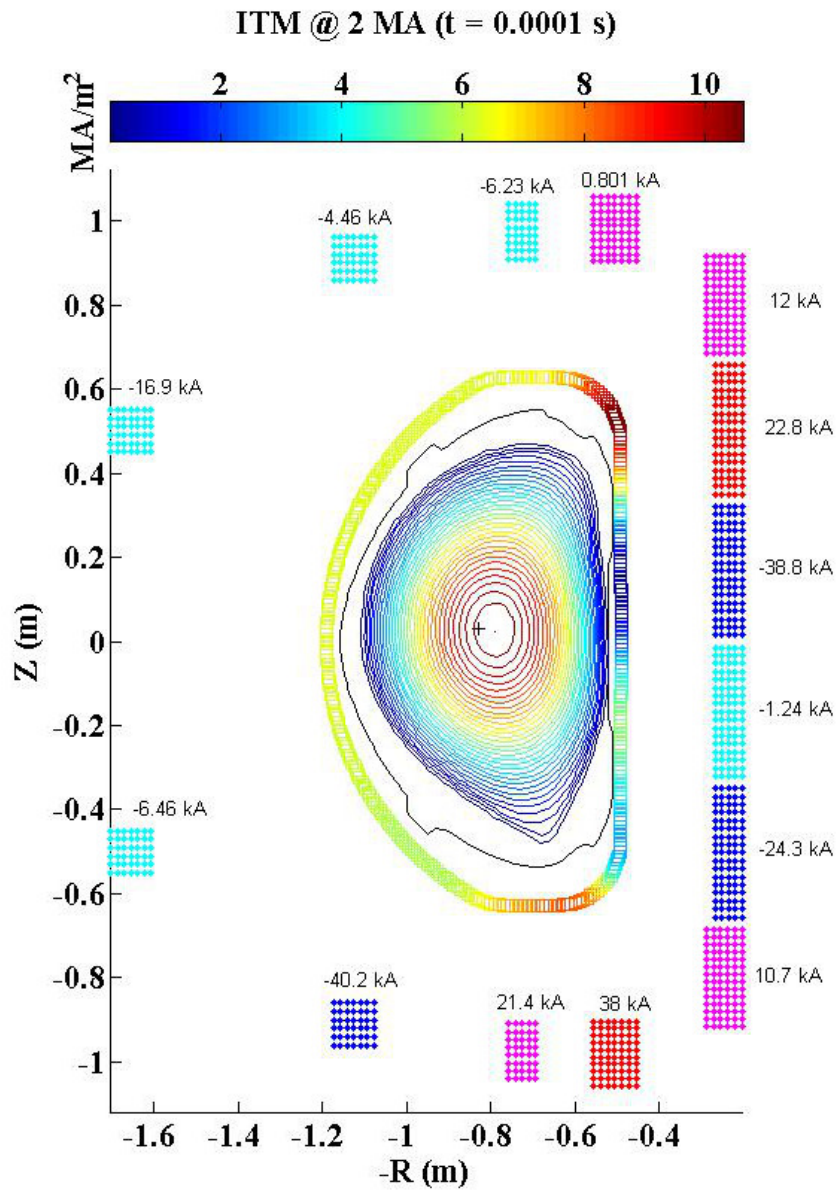


Figure 4.5: Plasma current density  $j_\phi$  (contours), poloidal field coils and the vessel structures of COMPASS-U calculated by FREEBIE inverse mode for D-shaped plasma with x-point.

## 4.2.2 Vertical Displacement Event

Starting with the static equilibria calculated in the previous section, FREEBIE can simulate the equilibrium time evolution. Any elongated plasma in a tokamak is vertically unstable and without a vertical feedback stabilization would the plasma column hit the wall and the discharge would end. This phenomenon can also be simulated by free-boundary equilibrium codes. On the contrary, circular plasmas are vertically stable. VDE is characterized by an exponential growth in the plasma vertical position. The growth rate may be interpreted as the time in which the plasma displacement grows by the coefficient of the euler constant  $e$ . VDE is usually characterized by a displacement in  $Z$  coordinate above a certain value, e.g. for mid-sized tokamaks approximately one centimetre. In order to construct properly fast vertical stabilization, the characteristic time of the VDE is needed.

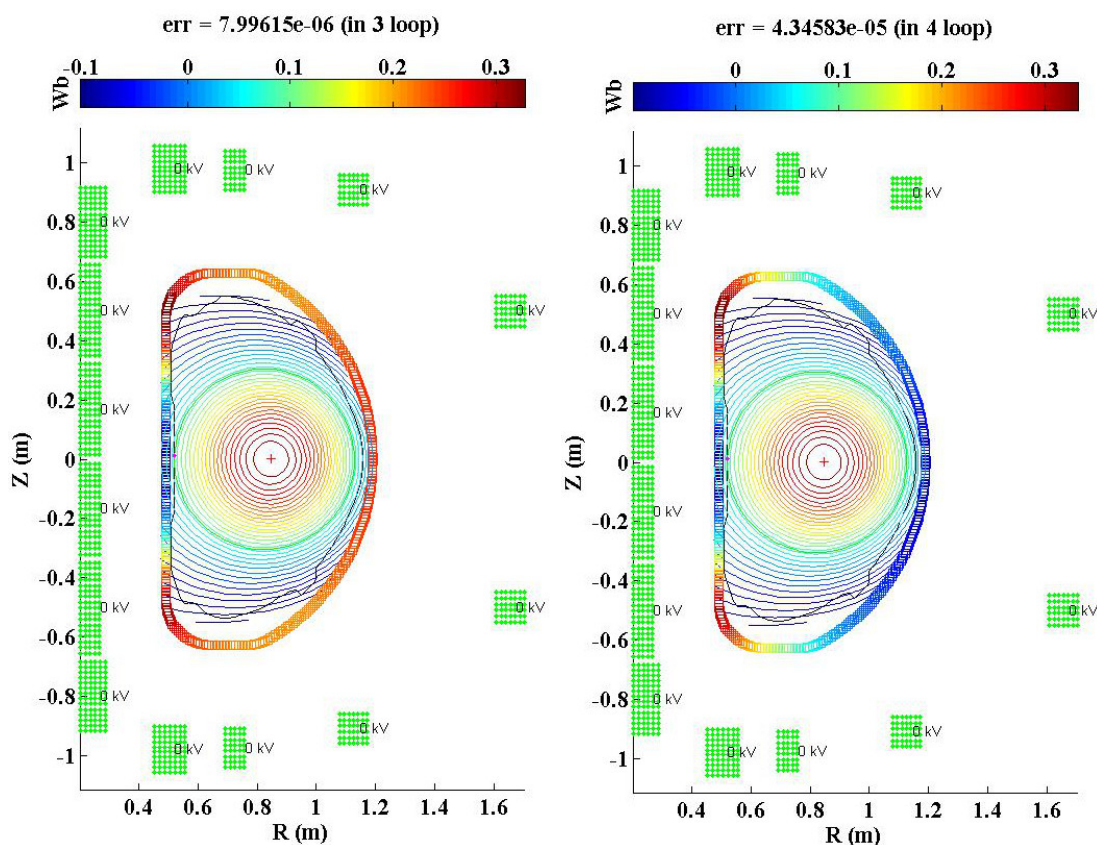


Figure 4.6: Equilibrium time evolution for a circular plasma. The left subfigure shows the initial state, i.e. after first step at  $t = 0.1s$ , and the state in  $t = 10ms$  is visualized in the right.

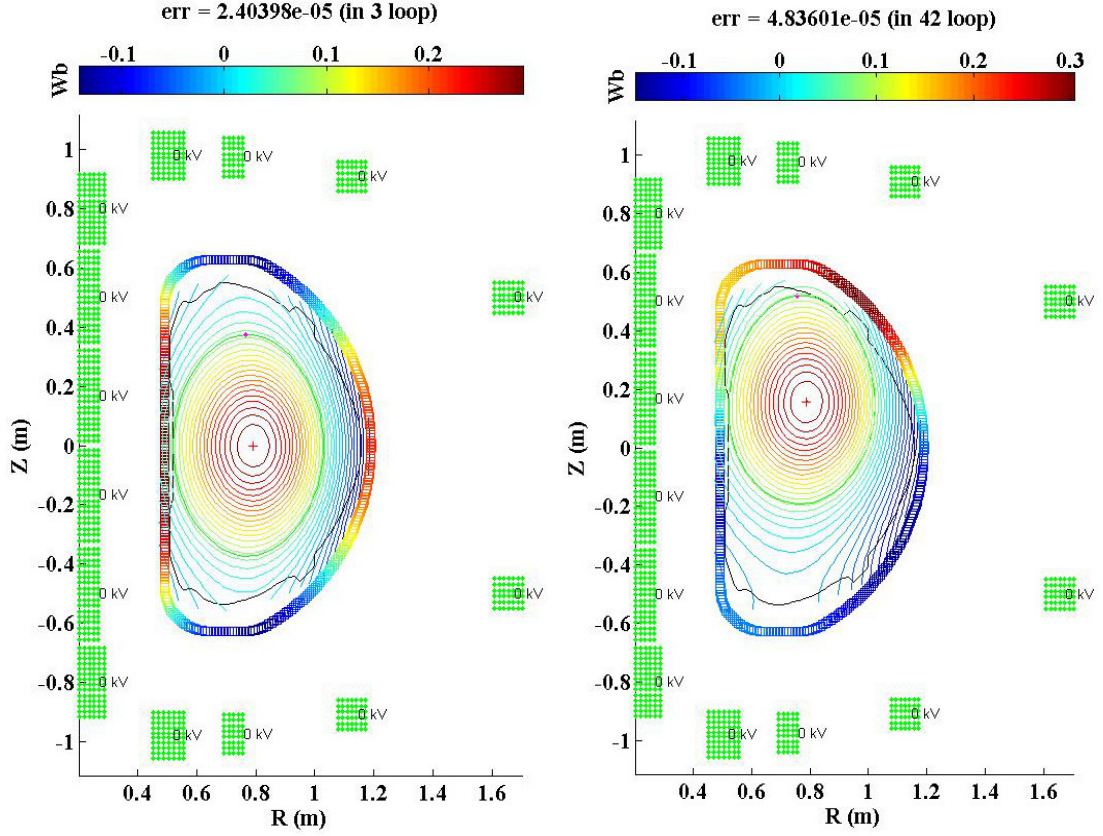


Figure 4.7: Visualisation of VDE for an elongated plasma shape. The left subfigure shows the initial state, i.e. after first step at  $t = 0.1s$ , and the state in  $t = 10ms$  is visualized in the right.

The VDE is simulated with usage of FREEBIE by turning off power supplies for the poloidal field coils when the plasma is in an equilibrium state and calculating in the time-evolution mode. The initial states for each plasma shapes considered in 4.2.1 and states after  $\Delta t = 10ms$  are visualized in figures 4.6, 4.7 and 4.8. More importantly, the  $Z$  coordinate of magnetic axis  $Z_{axis}$  data sets for individual calculations are plotted in the figure 4.9.

According to expectations, the circular plasma column is not unstable in the exponential way and its drift after  $\Delta$  is of order  $10^{-4}$ , i.e. smaller by two orders in comparison to elongated and shaped plasma. On the other hand, the vertical position evolution can easily be fitted by exponential functions:

$$\begin{aligned} f(t) &= -0.0008 + 0.0002 \exp(695t), \\ g(t) &= 0.03 - 0.002 \exp(390t), \end{aligned} \tag{4.9}$$

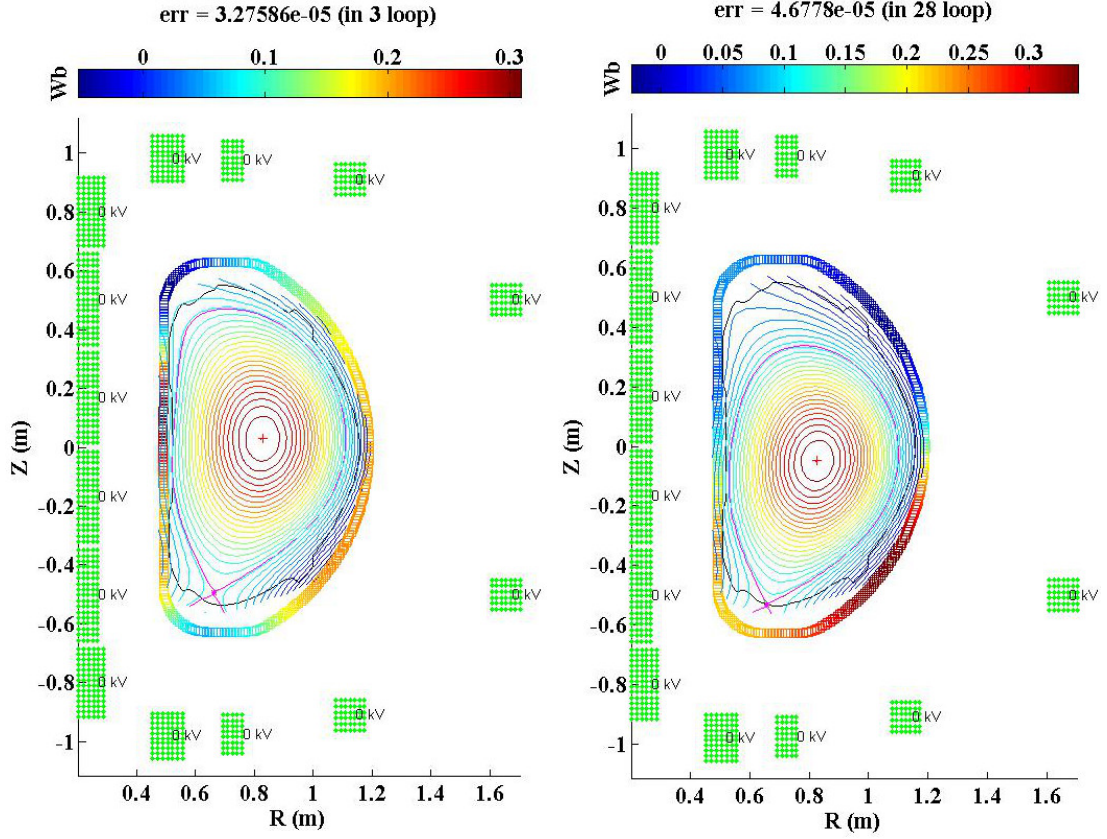


Figure 4.8: Visualisation of VDE for a shaped plasma with x-point. The left subfigure shows the initial state, i.e. after first step at  $t = 0.1s$ , and the state in  $t = 10 ms$  is visualized in the right.

for elongated and D-shaped plasma respectively.

The coefficients in exponentials are the characteristic growth rates of the VDE's and the resulting characteristic VDE times  $\tau_{elong}$  and  $\tau_{shaped}$  are

$$\begin{aligned}\tau_{elong} &= 1/695 = 1.44 ms, \\ \tau_{shaped} &= 1/390 = 2.56 ms,\end{aligned}\tag{4.10}$$

These time scales are important parameters for the vertical stabilization control of COMPASS-U.

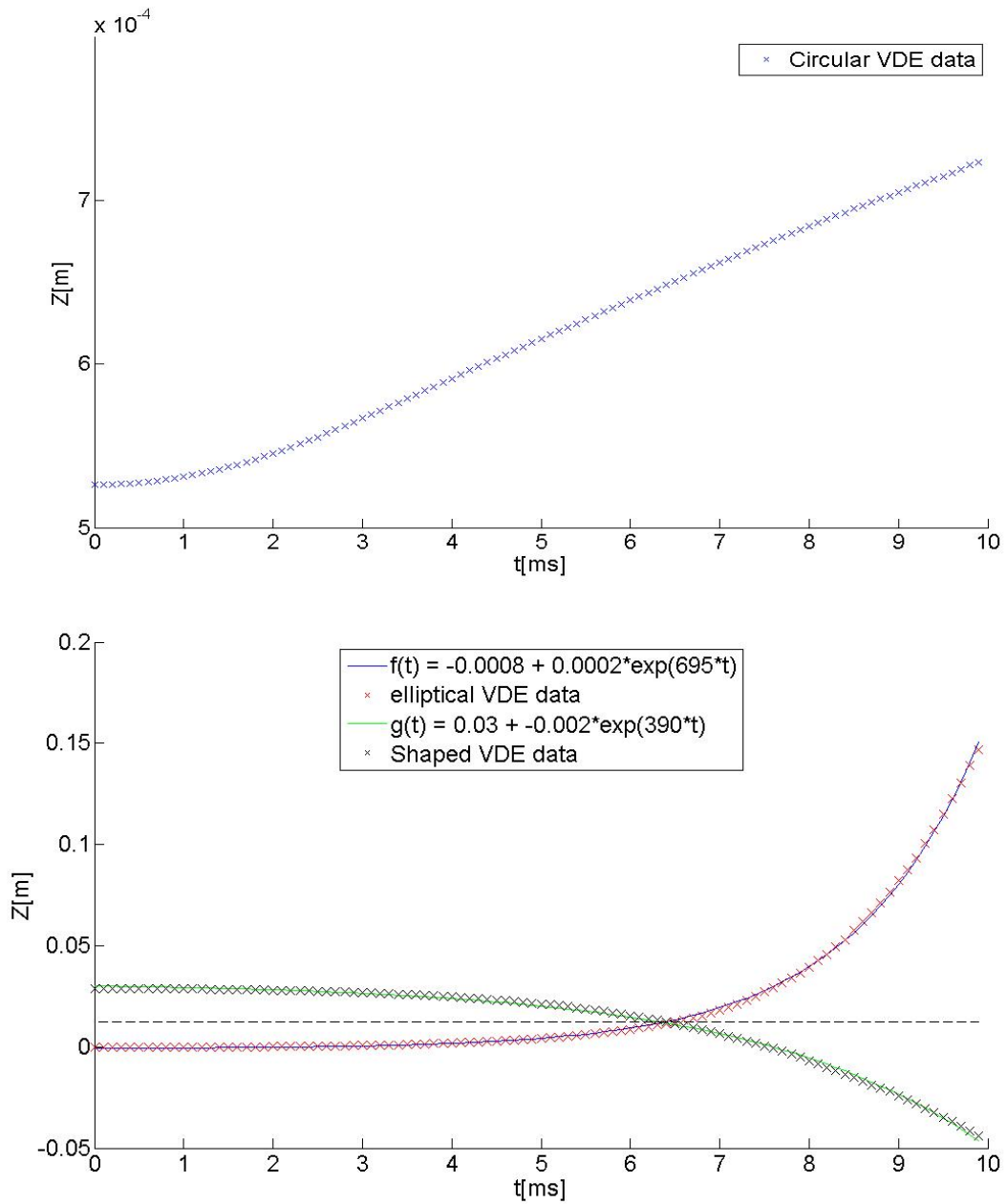


Figure 4.9: Evolution of z-coordinate of magnetic axis in time for circular, elongated and shaped plasma. Exponential dependencies are fitted by exponential functions  $f(t),g(t)$ , granting characteristic VDE times  $\tau_{elong} = 1/695 = 1.44 \text{ ms}$  and  $\tau_{shaped} = 1/390 = 2.56 \text{ ms}$  as a result.

### 4.3 Post-processing module `equi2D.py`

As the last enhancement of the calculation basis I have implemented a stand-alone post-processing module `equi2D.py`. The main motivation of this effort was the need for finding magnetic surfaces in poloidal cross-section of tokamak, i.e. equipotentials in 2-D function of  $\Psi$ . This tool is meant to be used to process equilibrium data. Its input is function  $\Psi$  calculated by any equilibrium solver. The core of all calculation done by the module is a equipotential finder of arbitrary function  $F(x, y)$  and its algorithm is derived in following text. The function  $F(x, y)$  does not have to be a continuous function, in fact it is meant to be mostly used for the function  $\Psi$  given on a grid as numerical result of any simulation. Data on a grid are in the module internally interpolated by high order spline and any values in the calculation are obtained as a evaluation of the spline.

In order to find a equipotential of a given function, the implicit function theory is first at hand to solve the challenge. Problem with the implicit solution is the turnarounds in specific coordinates, where the division by zero throws an error. This problem has an elegant workaround of additional dependency of coordinates [19]. The addition of one more variable in the system needs to be compensated by adding one more equation, giving the new variable a physical meaning. In our case, the dependency is on the variable  $\lambda$ , which is given the meaning of the equipotential length.

$$F(x, y) = 0, \quad (4.11)$$

$$\frac{\partial F}{\partial x} \frac{dx}{d\lambda} + \frac{\partial F}{\partial y} \frac{dy}{d\lambda} = 0, \quad (4.12)$$

$$(d\lambda)^2 = (dx)^2 + (dy)^2, \quad (4.13)$$

where  $F(x, y)$  is in general the described 2-D function with dependency on its coordinates  $x, y$ , which has further dependency on the curve length  $\lambda$ . By separating the proper derivations, a set of equations for each coordinate is obtained

$$\frac{dx}{d\lambda} = \mp \frac{F_y}{\sqrt{F_x^2 + F_y^2}}, \quad x(0) = x_0, \quad (4.14)$$

$$\frac{dy}{d\lambda} = \pm \frac{F_x}{\sqrt{F_x^2 + F_y^2}}, \quad y(0) = y_0, \quad (4.15)$$

where  $F_x, F_y$  are derivatives of the function  $F$  by  $x$  or  $y$  coordinate respectively.

By evaluating these equations, which cannot in normal cases encounter the division by zero, the problem is solved.

In special case of the tokamak application, the function  $F$  is equivalent to the function  $\Psi$  and coordinates are  $R, Z$ . This special case was used to benchmark the algorithm to the contour plot function of `matplotlib.pyplot` package (fig.4.10). The algorithm itself is written as an python stand-alone package imported.

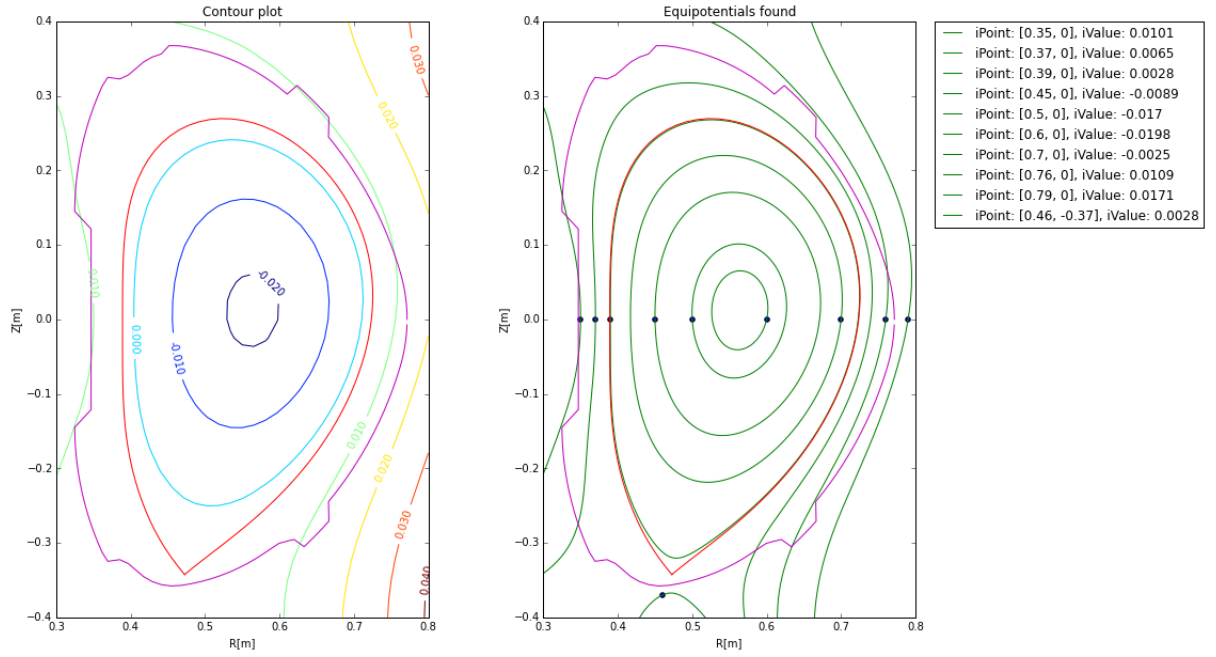


Figure 4.10: Comparison of contour plot(left) and algorithm results(right); The function shown is  $\Psi(R, Z)$  in tokamak COMPASS, the purple line visualizes the tokamak chamber and the red one is the last closed flux surface (LCFS).

Apart from the equipotential finder core the module consists of various calculation procedures, i.e. calculation of volume enclosed by given magnetic surface<sup>3</sup> and the area of the magnetic surface, calculation of separatrix position and averaging a variable over the magnetic surface. It could be furthermore extended by a function for coordinates transformation.

<sup>3</sup>This feature is especially useful for NBI studies by the METIS calculations.

# Summary

This thesis documents an effort of enhancement of equilibrium solver module FREEBIE by a solver of general electrical circuits. The solver itself was created and verified on several simple, analytically solved circuits. Its behaviour for complex circuits, in particular for the COMPASS poloidal field power supply system, follows expectations. The original goal of integration of the solver into the FREEBIE module was not fully finished because of technical complications.

In order to enhance the COMPASS tokamak lifetime and relevance in the tokamak physics studies, an upgrade to the COMPASS-U device is considered. The contribution of this work for the COMPASS-U design procedure has two steps. At first, simulations of static equilibria for representative plasma shapes were calculated. These calculations confirmed that these plasma shapes can be created by the current PF coils design. The calculated currents in the PF coils specify minimal requirements on the COMPASS-U PF systems.

In the second step, the static equilibria are evolved in time without any feedback stabilization. The results confirmed the stability of circular plasmas. For elongated plasmas, vertical displacement events were simulated and characterized. By fitting the vertical position evolution by an exponential function data, the VDE growth rates were estimated. The growth rates imply limits on the time response of vertical stabilization at COMPASS-U. The lowest value observed in these simulations was

$$\tau = 1.44 \text{ ms.}$$

As the calculation basis missed a stand-alone post-processing module, it was implemented as part of this work and is now actively used at the COMPASS tokamak. The module of name `equi2D.py` consist of equipotential finder as the core function and several other functions processing independent tasks, e.g. calculation of the volume enclosed by a magnetic flux circuit given by input point  $(R_0, Z_0)$ . The equipotential finder was benchmarked for the python `matplotlib.pyplot` module's function `contour plot` with similar visual result. The importance of the stand-alone solver and the rest of the module is its speed of computation, easy way of retrieving specific data and most importantly usage of general spline class. This way grants possible future consistency by the unified data handling between the `equi2D.py` module and other calculation codes.

# Bibliography

- [1] J. Šafránková, ed. *20th Annual Conference of Doctoral Students, WDS'11 "Week of Doctoral Students 2011"*, Charles University, Faculty of Mathematics and Physics, Prague, Czech Republic, May 31, 2011 to June 3, 2011.: [proceedings of contributed papers]. Pt. 2: *Physics of plasmas and ionized media*. Vyd. 1. Praha: Matfyzpress, 2011. 282 s. ISBN: 978-80-7378-185-9.
- [2] R AMROLLAHI. "Green Function of Axisymmetric Magnetostatics". In: *Iranian Journal of Science and Technology (Sciences)* 28.2 (2004), s. 197–204.
- [3] J.F. Artaud a S.H. Kim. "A new free-boundary equilibrium evolution code, FREEBIE". Conference talk. 39th EPS Conference & 16th Int. Congress on Plasma Physics. Stockholm, Sweden, 2012.
- [4] George E. P. Box a Norman Richard Draper. *Empirical model-building and response surfaces*. Wiley series in probability and mathematical statistics. New York: Wiley, 1987. 669 s. ISBN: 978-0-471-81033-9.
- [5] Francis F Chen. *Introduction to Plasma Physics and Controlled Fusion Volume 1: Plasma Physics*. Boston, MA: Springer US, 1984. ISBN: 978-1-4757-5595-4. URL: <http://dx.doi.org/10.1007/978-1-4757-5595-4> (cit. 05.05.2016).
- [6] David P. Coster et al. "The European Transport Solver". In: *IEEE Transactions on Plasma Science* 38.9 (zář. 2010), s. 2085–2092. ISSN: 0093-3813. DOI: 10.1109/TPS.2010.2056707. URL: <http://ieeexplore.ieee.org/document/5547593/> (cit. 09.01.2017).
- [7] G. Cunningham. "High performance plasma vertical position control system for upgraded MAST". In: *Fusion Engineering and Design* 88.12 (pros. 2013), s. 3238–3247. ISSN: 09203796. DOI: 10.1016/j.fusengdes.2013.10.001. URL: <http://linkinghub.elsevier.com/retrieve/pii/S0920379613006753> (cit. 06.05.2016).
- [8] G.L. Falchetto et al. "The European Integrated Tokamak Modelling (ITM) effort: achievements and first physics results". In: *Nuclear Fusion* 54.4 (1.dub. 2014), s. 043018. ISSN: 0029-5515, 1741-4326. DOI: 10.1088/0029-5515/54/4/043018. URL: <http://stacks.iop.org/0029-5515/54/i=4/a=043018?key=crossref.d4d2924c154ff8df0155803f67b5d6a0> (cit. 03.05.2016).

- [9] Jeffrey P. Freidberg. *Plasma physics and fusion energy*. Cambridge: Cambridge University Press, 2007. 671 s. ISBN: 978-0-521-85107-7 978-0-521-73317-5.
- [10] J. P. Goedbloed a Stefaan Poedts. *Principles of magnetohydrodynamics: with applications to laboratory and astrophysical plasmas*. Cambridge, UK ; New York: Cambridge University Press, 2004. 613 s. ISBN: 978-0-521-62347-6 978-0-521-62607-1.
- [11] *GOLEM @ FJFI.CVUT*. URL: <http://golem.fjfi.cvut.cz/> (cit. 06.05.2016).
- [12] H. Heumann et al. “Quasi-static free-boundary equilibrium of toroidal plasma with CEDRES++: Computational methods and applications”. In: *Journal of Plasma Physics* 81.3 (červ. 2015). ISSN: 0022-3778, 1469-7807. DOI: 10.1017/S0022377814001251. URL: [http://www.journals.cambridge.org/abstract\\_S0022377814001251](http://www.journals.cambridge.org/abstract_S0022377814001251) (cit. 06.05.2016).
- [13] F. Imbeaux et al. “Design and first applications of the ITER integrated modelling & analysis suite”. In: *Nuclear Fusion* 55.12 (1.lis. 2015), s. 123006. ISSN: 0029-5515, 1741-4326. DOI: 10.1088/0029-5515/55/12/123006. URL: <http://stacks.iop.org/0029-5515/55/i=12/a=123006?key=crossref.e736dfd9476f9898542f271> (cit. 09.01.2017).
- [14] S. C. Jardin. “Some Considerations and Techniques for the Predictive Simulation of Global Instabilities in Tokamaks”. In: *Fusion Science and Technology* 59.3 (dub. 2011), s. 519–525.
- [15] Stephen Jardin. *Computational methods in plasma physics*. Boca Raton, FL: CRC Press/Taylor & Francis, 2010. ISBN: 978-1-4398-1095-8. URL: <http://www.crcnetbase.com/isbn/9781439810958> (cit. 24.02.2016).
- [16] J.Urban a J.-F.Artaud. *Coupled Transport and Free-boundary Equilibrium Simulations using FREEBIE and CRONOS*. 2012.
- [17] Jindřich Kocman. “Zpětnovazební řízení polohy na tokamaku GOLEM”. Dis. Czech Technical University in Prague, 2011. URL: [http://physics.fjfi.cvut.cz/publications/FTTF/BP\\_Jindrich\\_Kocman.pdf](http://physics.fjfi.cvut.cz/publications/FTTF/BP_Jindrich_Kocman.pdf).
- [18] Petr Kulhánek. *Úvod do teorie plazmatu*. Praha: AGA, 2011. ISBN: 978-80-904582-2-2.
- [19] E.B. Kuznetsov. “Optimal parametrization in numerical construction of curve”. In: *Journal of the Franklin Institute* 344.5 (2007), s. 658–671.
- [20] Martin Libra, Jan Mlynář, Vladislav Poulek a Česká zemědělská univerzita v Praze. *Jaderná energie*. Praha: Ilsa, 2012. ISBN: 978-80-904311-6-4.
- [21] Matusu, M. J. “Modelling of magnetic equilibrium in tokamaks”. Dis. Prague: Czech Technical University in Prague, 2015. URL: [http://physics.fjfi.cvut.cz/publications/FTTF/VU\\_Martin\\_Matusu.pdf](http://physics.fjfi.cvut.cz/publications/FTTF/VU_Martin_Matusu.pdf) (cit. 06.05.2016).
- [22] *plazmak2010.jpg (1256x1121)*. URL: <http://www.szfkj.hu/images/lphys/plazmak2010.jpg> (cit. 05.05.2016).

- [23] *Toroidal coordinates - FusionWiki*. URL: [http://fusionwiki.ciemat.es/wiki/Toroidal\\_coordinates](http://fusionwiki.ciemat.es/wiki/Toroidal_coordinates) (cit. 05.05.2016).
- [24] ITER Physics Expert Group on Confin Transport, ITER Physics Expert Group on Confin Database a ITER Physics Basis Editors. “Chapter 2: Plasma confinement and transport”. In: *Nuclear Fusion* 39.12 (pros. 1999), s. 2175–2249. ISSN: 0029-5515. DOI: 10.1088/0029-5515/39/12/302. URL: <http://stacks.iop.org/0029-5515/39/i=12/a=302?key=crossref.c457c1e0ef9f22c2316445d85184a82d> (cit. 05.05.2016).
- [25] J. Urban et al. “Free-boundary equilibrium transport simulations of ITER scenarios under control”. In: 39th EPS Conference & 16th Int. Congress on Plasma Physics. Sv. 36F. Stockholm, Sweden: European Physical Society, 2012, P1.019.